General Disclaimer

One or more of the Following Statements may affect this Document

- This document has been reproduced from the best copy furnished by the organizational source. It is being released in the interest of making available as much information as possible.

- This document may contain data, which exceeds the sheet parameters. It was furnished in this condition by the organizational source and is the best copy available.

- This document may contain tone-on-tone or color graphs, charts and/or pictures, which have been reproduced in black and white.

- This document is paginated as submitted by the original source.

- Portions of this document are not fully legible due to the historical nature of some of the material. However, it is the best reproduction available from the original submission.

N O T I C E

EFFECT OF WING-TRANSITION LOCATION
AND SLOTTED AND UNSLOTTED FLAPS ON
AERODYNAMIC CHARACTERISTICS OF A
FIGHTER MODEL AT HIGH SUBSONIC SPEEDS

by Theodore G. Ayers

Langley Research Center
Langley Station, Hampton, Va.

EFFECT OF WING-TRANSITION LOCATION AND
SLOTTED AND UNSLOTTED FLAPS ON AERODYNAMIC CHARACTERISTICS
OF A FIGHTER MODEL AT HIGH SUBSONIC SPEEDS*

By Theodore G. Ayers
Langley Research Center

SUMMARY

An investigation has been conducted in the Langley 8-foot transonic pressure tunnel to determine the effects of wing-transition location and of slotted and unslotted full-span flaps on the longitudinal aerodynamic characteristics of a 1/15-scale model of a variable-wing-sweep tactical fighter model at Mach numbers from 0.70 to 0.85 for a wing leading-edge sweep of 26°.

The results of this investigation have indicated that moving the wing-transition trip rearward to simulate the full-scale boundary-layer characteristics had little effect on the subcritical aerodynamics of the model. At higher Mach numbers where supercritical flow exists and shock-induced separation occurs, the lift and pitching-moment characteristics were substantially altered to provide increases in the lift coefficient (at constant angle of attack) and static margin of stability of the configuration resulting from the thinner boundary layer, and more rearward wing shock-wave location for the aft transition-trip location. Because existing wing constraints precluded optimizing the configuration, no improvement was noted in the cruise efficiency for the model with the 4° slotted flaps as compared with that for the basic configuration. The use of slotted flaps did, however, provide substantial improvements in the lift-drag ratio at the cruise lift for Mach numbers above 0.80 and throughout the Mach number range at lift coefficients greater than 0.50. The use of the 4° unslotted flap increased the cruise efficiency of the basic configuration by about 3 percent at Mach 0.79, the highest Mach number for which data were obtained with unslotted flaps. Increasing the flap deflection to 8° resulted in substantial drag penalties at and below the cruise lift coefficient as compared with those for the basic or the 4° unslotted flap configuration. All the configurations with flap deflections show an increase in usable lift coefficient and increased static margin at the higher Mach numbers resulting from the more rearward center-of-pressure location and the delay in the onset of wing-flow separation, the slotted flap generally providing the greatest increase.

---

*Title Unclassified.

INTRODUCTION

The present investigation is part of a more general research program intended to provide information for the development of variable-wing-sweep multimission airplane configurations. The results of some previous studies can be found in references 1 to 4.

Recent research directed toward improving the aerodynamic efficiency of wings through the use of the slotted supercritical airfoil (ref. 5) has shown very promising results. Based on these results, a program was initiated whereby the slotted super-critical airfoil was approximated by utilizing the flap system of a model of an existing variable-wing-sweep tactical fighter airplane. The results included herein were obtained to evaluate the effects of wing-transition location and full-span slotted and unslotted flaps on the longitudinal aerodynamic characteristics of the model with 26° wing leading-edge sweep.

SYMBOLS

The results as presented herein are referred to the stability-axes system. The moment center was located along the model reference line at a point 88.278 centimeters rearward of the nose (0.45 mean aerodynamic chord). (See fig. 1.) All coefficients are based on the geometry of the wing with a leading-edge sweep angle of 16°.

C_D drag coefficient, $\dfrac{\text{Drag}}{qS}$

$C_{D,i}$ internal drag coefficient, $\dfrac{\text{Internal drag}}{qS}$

C_L lift coefficient, $\dfrac{\text{Lift}}{qS}$

C_m pitching-moment coefficient, $\dfrac{\text{Pitching moment}}{qS\bar{c}}$

$C_{m_{C_L}}$ longitudinal-stability derivative, $\dfrac{C_m}{C_L}$ $\left(C_L \approx 0.5\right)$

$\bar{c}$ wing mean aerodynamic chord, 18.372 cm

L/D   lift-drag ratio

M   free-stream Mach number

$p_{t,\infty}$ free-stream stagnation pressure, N/m^2

q   free-stream dynamic pressure, N/m^2

S   wing area including fuselage intercept, 0.217 meter^2

α angle of attack referenced to wing chord plane, deg

δ_s wing spoiler deflection, positive when trailing edge is up   (Subscripts denote spoiler segments shown in fig. 2), deg

δ_{fr} wing trailing-edge flap rotation, positive when trailing edge is down, deg

δ_{ft} wing trailing-edge flap-track rotation, positive when trailing edge is down, deg

Λ leading-edge sweep of outboard wing panel, deg

MODEL DESCRIPTION

The model used in the present investigation was a 1/15-scale model of a twin-engine variable-wing-sweep tactical fighter configuration. The general arrangement and details of the model are presented in figures 1 to 3. Although provision was made for varying the wing leading-edge sweep from 16° to 72.5^o, only the 26° sweep configuration was tested during the present investigation. The model was of the inboard-wing-pivot type with the pivot located longitudinally 82.643 cm aft of the model nose and laterally 11.905 cm outboard of the model plane of symmetry.

The wing, which was mounted at 1° positive incidence with respect to the model reference line, consisted of modified NACA 64A series airfoils outboard of the wing pivot and parallel to the free stream ($\Lambda = 16^o$). The wing varied in thickness from about 12-percent chord at the pivot to about 9-percent chord at the tip. In addition, the wing was uniformly twisted about the 26.146-percent chord line; the twist varied from 0° at the pivot to -4° at the tip.

The airplane landing-flap system, except for the leading-edge devices, was incorporated into the model and consisted of a 22-percent chord, four-segment spoiler system and a 28.5-percent-chord double slotted trailing-edge flap with the appropriate brackets to simulate the desired flap settings for either a simple flap rotation or a more complex Fowler type flap rotation along a circular arc track. (See figs. 2 and 3.) For the data presented herein, the flap vane was constructed as an integral part of the spoiler system as shown in section A-A of figure 2. The sketches in figure 3 show the four wing configurations that were investigated. The slotted airfoil shown in this figure was an attempt

to approximate the supercritical airfoil concept (see ref. 5) with a minimum modification to the basic wing geometry. For this configuration the trailing-edge flap was rotated 4° along the circular-arc track $\left(\delta_{ft} = 4^O\right)$ to provide a slotted airfoil; the three inboard spoilers were deflected up 3° to reduce the upper surface curvature of the airfoil ahead of the slot, and the vane and air director door were positioned to provide the desired slot and slot entrance shape. The two unslotted airfoil shapes were obtained by simple flap rotations of 4° and 8° $\left(\delta_{fr} = 4^O \text{ and } \delta_{fr} = 8^O\right)$, that is, rotation about the center of curvature of the flap upper surface.

The horizontal tails which were mounted on the model with 1^O positive incidence and 1^O negative dihedral consisted of biconvex airfoil sections parallel to the free stream and varied in thickness from 4-percent chord at the root to 3-percent chord at the tip. The vertical tail consisted of 3.2-percent-thick modified biconvex airfoil sections parallel to the free stream. Twin ventral fins were mounted on the lower aft fuselage and canted outward 30° from the model plane of symmetry.

APPARATUS AND PROCEDURES

Tunnel

The tests were conducted in the Langley 8-foot transonic pressure tunnel which is a single-return tunnel having a rectangular slotted test section to permit continuous operation through the transonic speed range with negligible choking and blockage effects. The stagnation pressure was varied, as shown in figure 4, to maintain a constant Reynolds number per meter of 1.07×10^6.

Boundary-Layer Transition

During the tests two wing transition-trip locations were investigated. The first, referred to herein as transition location 1, consisted of 0.25-cm-wide strips of No. 120 carborundum grains located 1.52 cm streamwise aft of the leading edge of the wing, horizontal and vertical tail surfaces, and inlets and No. 80 carborundum grains 3.81 cm rearward from the model nose. Transition location 2 was the same as location 1 except for the outer wing panels. For transition location 2, the trips on the outer wing panels were located by using the techniques discussed in references 6 and 7 to simulate the full-scale Reynolds number boundary-layer separation characteristics. Transition location 2 for the basic wing with and without unslotted flaps consisted of 0.25-cm-wide strips of No. 100 carborundum grains located at 40 and 45 percent of the local chord on the wing upper and lower surfaces, respectively. The wing with the slotted flap was the same except that transition was also fixed on the flap upper and lower surfaces by applying 0.25-cm-wide strips of No. 180 and No. 150 carborundum grains, respectively, at the 50-percent flap chord.

Measurements

Six-component static aerodynamic force and moment measurements were obtained by means of an electrical strain-gage balance located within the fuselage cavity. The measurements were taken over an angle-of-attack range from about 0° to 10° at Mach numbers from 0.70 to 0.85. All data were obtained for a wing leading-edge sweep of 26°. Static pressures were measured at the balance chamber and nozzle exit plug bases.

Corrections

The drag coefficient C_D has been corrected for flow through the engine ducts. The variation of the internal drag coefficients $C_{D,i}$ with angle of attack is shown in figure 5 for both ducts. The drag data have been adjusted to the condition of free-stream static pressure acting over the balance cavity and nozzle exit plug bases.

The measured angles of attack have been corrected for model support sting and balance deflections occurring upstream of the angle measurement device as the result of aerodynamic loads on the model. The angles of attack are estimated to be accurate within $\pm 0.1^O$; the Mach number, within ± 0.002.

PRESENTATION OF RESULTS

The results of this investigation are presented in the following figures:

DISCUSSION OF RESULTS

Effects of Transition Location

The effects of the wing-transition location on the longitudinal aerodynamic characteristics of the basic configuration are presented in figure 6. In general, moving the wing-transition trips from location 1 to location 2 had little effect on the subcritical aerodynamics of the model other than some negative shift in the pitching-moment characteristics and

lower drag levels associated with the greater chordwise run of laminar flow over the wing. At the higher Mach numbers where supercritical flow exists and shock-induced separation occurs (M = 0.79 to 0.85), there are significant differences in the lift and pitching-moment results as well as the expected differences in drag levels because of the increased chordwise laminar flow. For example, at a Mach number of 0.85 (fig. 6(e)), the results obtained for transition location 2 show the model to be longitudinally stable in the lift-coefficient range from 0 to about 0.40 whereas the results for transition location 1 indicate the model to be longitudinally unstable throughout this same lift-coefficien' range. In addition, the lift coefficient obtained for transition location 2 at $\alpha = 4^O$ is about 18 percent higher than that obtained with transition location 1. These resulting increases in both lift coefficient and stability level obtained for transition location 2 are associated with the thinner boundary layer and more rearward location of the wing shock wave. As is reported in references 6 and 7, proper placement of the transition trip (transition location 2) should result in a reasonably good approximation of the full-scale boundary-layer-separation characteristics.

Effects of Cruise Flaps

The effects of the slotted and unslotted flaps on the longitudinal characteristics of the model with transition location 2 are presented in figures 7 and 8 and the drag characteristics are summarized in figure 9 for a cruise lift coefficient of 0.50. As was stated previously, the slotted cruise flap was an attempt to approximate the slotted supercritical airfoil described in reference 1 with minimum modification to the existing airplane wing. (See fig. 3.) However, because of the existing wing constraints, the full potential of the supercritical airfoil concept could not be realized. The increased wetted area of the slot and the severe aerodynamic obstructions of the flap tracks resulted in a subcritical drag level for the slotted configuration which was significantly higher than that of the basic configuration. At the design condition, M = 0.80 and C_L = 0.5, the drag levels of the two configurations were essentially the same. It should be pointed out, however, that the drag increment between the basic and the slotted-flap configuration would be reduced when extrapolating the data to full-scale conditions because of the much lower effective Reynolds number on the flap at the model test conditions. Further reductions in this drag increment could be realized by aerodynamic improvements to the flap-track system on the airplane. Although the use of the slotted flap did not improve the range factor (M × L/D) at the design point of M = 0.80 and C_L = 0.5, the data of figure 7 show an improvement in lift-drag ratio at C_L = 0.5 for Mach numbers above 0.8 and for all higher lift coefficients throughout the Mach number range for which data were obtained. These improvements are the result of a delay in shock-induced separation for the slotted-flap configuration. Also summarized in figure 9 are the cruise drag characteristics for the model with unslotted flaps having 4° and 8° of simple flap rotation, that is, rotation about the

center of curvature of the flap upper surface. Because time considerations precluded testing the unslotted flaps at Mach numbers beyond 0.79 (see fig. 8(d)), no comparison can be made with the basic or slotted flaps at the design point. The data obtained for the 4° unslotted flap at M = 0.79 do, however, indicate about a 3-percent improvement in range factor as compared with the basic configuration. (See fig. 9.) The unslotted flaps provide significant improvements over the basic configuration at higher lift coefficients throughout the Mach number range for which data were obtained.

The pitching-moment characteristics for the basic and slotted-flap configurations are presented in figure 7. As would be expected, the slotted flap results in a more negative pitching-moment level because of the more rearward center-of-pressure location on the wing. Of more significance, however, is the substantial increase in usable lift coefficient (delay in pitch-up) at Mach numbers of 0.79 and above for the slotted-flap configuration which results from a delay in the onset of wing flow separation. These trends are generally the same for the model with unslotted flaps (see fig. 8) although the indicated increase in usable lift coefficient is not so large as that for the model with the 4° slotted flap. The longitudinal stability characteristics are summarized in figure 10 for a lift coefficient of 0.50. All the flap configurations show considerable improvement over the basic configuration at Mach numbers between 0.75 and 0.85, some reduction in the static margin of stability being noted for the 4° slotted and unslotted flaps at a Mach number of 0.70.

CONCLUSIONS

An investigation has been conducted in the Langley 8-foot transonic pressure tunnel to determine the effects of wing-transition location and of slotted and unslotted full-span flaps on the longitudinal aerodynamic characteristics of a 1/15-scale model of a variable-wing-sweep tactical fighter model at Mach numbers from 0.70 to 0.85 for a wing leading-edge sweep of 26°. The following conclusions are indicated:

1. Moving the wing-transition trip rearward to simulate the full-scale boundary-layer characteristics had little effect on the subcritical aerodynamics of the model other than a negative shift in the pitching-moment coefficient and the expected drag reduction. At higher Mach numbers where supercritical flow exists and shock-induced separation occurs, the lift and pitching-moment characteristics were substantially altered to provide increases in both the lift coefficient, at constant angle of attack, and static margin of the configuration resulting from the thinner boundary layer and more rearward wing-shock-wave location for the aft transition-trip location.

2. Because existing wing constraints precluded optimizing the configurations no improvement was noted, at wind-tunnel Reynolds numbers, in the cruise efficiency for the model with the 4° slotted flaps as compared with that for the basic configuration. The

use of slotted flaps did, however, provide substantial improvements in lift-drag ratio at the cruise lift for Mach numbers above 0.80 and throughout the Mach number range at lift coefficients greater than 0.50.

3. The use of the 4° unslotted flap provided an increase in the cruise efficiency of the basic configuration of about 3 percent at Mach 0.79, the highest Mach number for which data were obtained with unslotted flaps.

4. Increasing the unslotted flap deflection to 8° resulted in substantial drag penalties at and below the cruise lift coefficient, as compared with those for the basic and 4° unslotted flap configuration.

5. All the configurations with flap deflections showed an increase in usable lift coefficient and increased static margin of stability at the higher Mach numbers resulting from the more rearward center-of-pressure location and the delay in wing flow spearation, the slotted flap generally providing the greatest increase.

Langley Research Center,
  National Aeronautics and Space Administration,
    Langley Station, Hampton, Va., May 20, 1969,
      720-01-00-18-23.

REFERENCES

1. Ayers, Theodore G.: Transonic Aerodynamic Characteristics of a Variable-Wing-Sweep Tactical Fighter Model – Phase 3. NASA TM X-1183, 1965.

2. Ayers, Theodore G.: Transonic Aerodynamic Characteristics of a Variable-Wing-Sweep Tactical Fighter Model – Phase 4. NASA TM X-1237, 1966.

3. Ayers, Theodore G.: Transonic Aerodynamic Characteristics of a Variable-Wing-Sweep Tactical Fighter Model – Phase 5. NASA TM X-1368, 1967.

4. Ayers, Theodore G.: Transonic Aerodynamic Characteristics of a Variable-Wing-Sweep Tactical Fighter Model – Phase 6. NASA TM X-1523, 1968.

5. Whitcomb, Richard T.; and Clark, Larry R.: An Airfoil Shape for Efficient Flight at Supercritical Mach Numbers. NASA TM X-1109, 1965.

6. Loving, Donald L.: Wind-Tunnel—Flight Correlation of Shock-Induced Separated Flow. NASA TN D-3580, 1966.

7. Blackwell, James A., Jr.: Preliminary Study of Effects of Reynolds Number and Boundary-Layer Transition Location on Shock-Induced Separation. NASA TN D-5003, 1969.
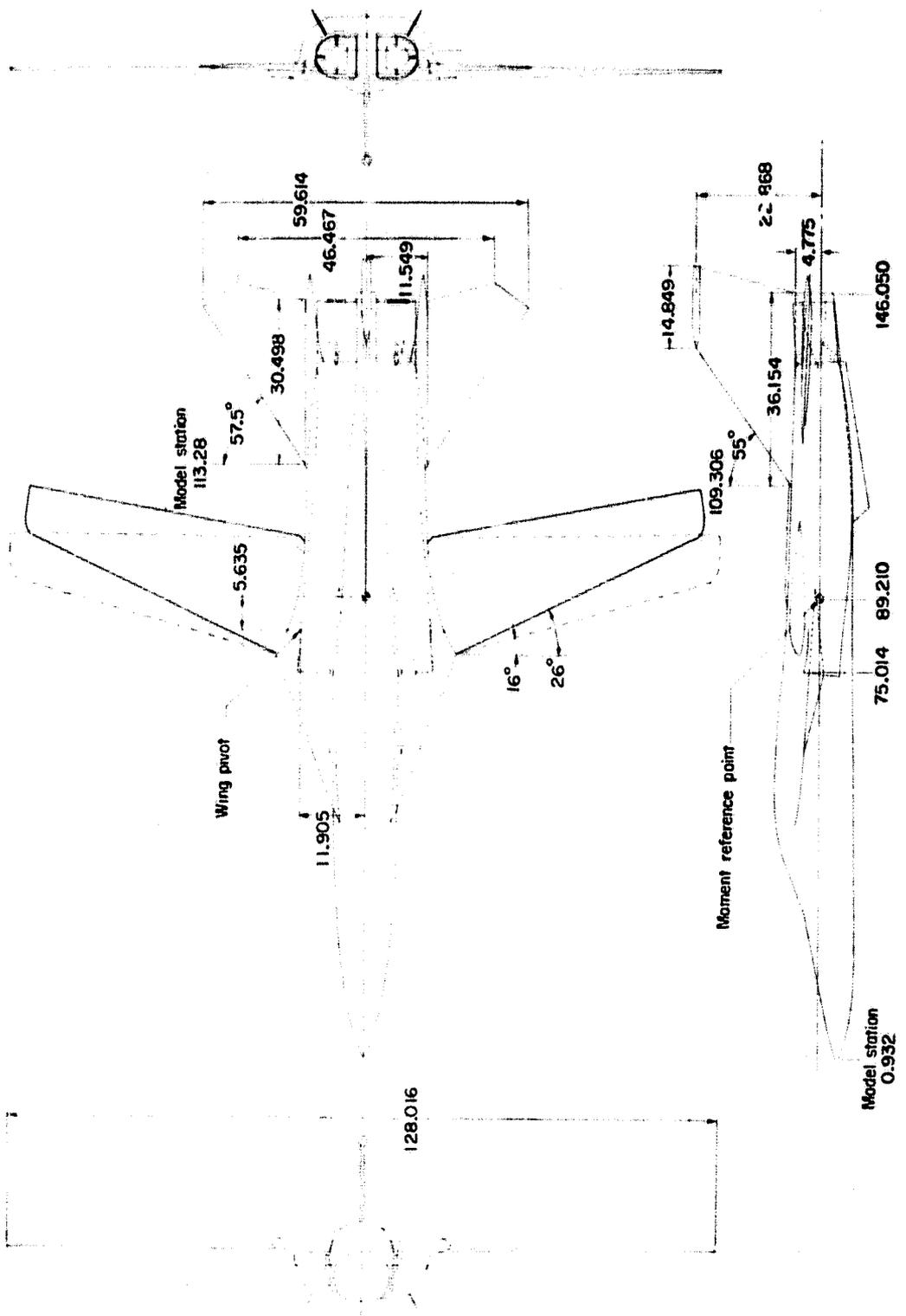
Figure 1.- Arrangement of 1/15-scale variable-wing-sweep fighter model. All linear dimensions are in centimeters.
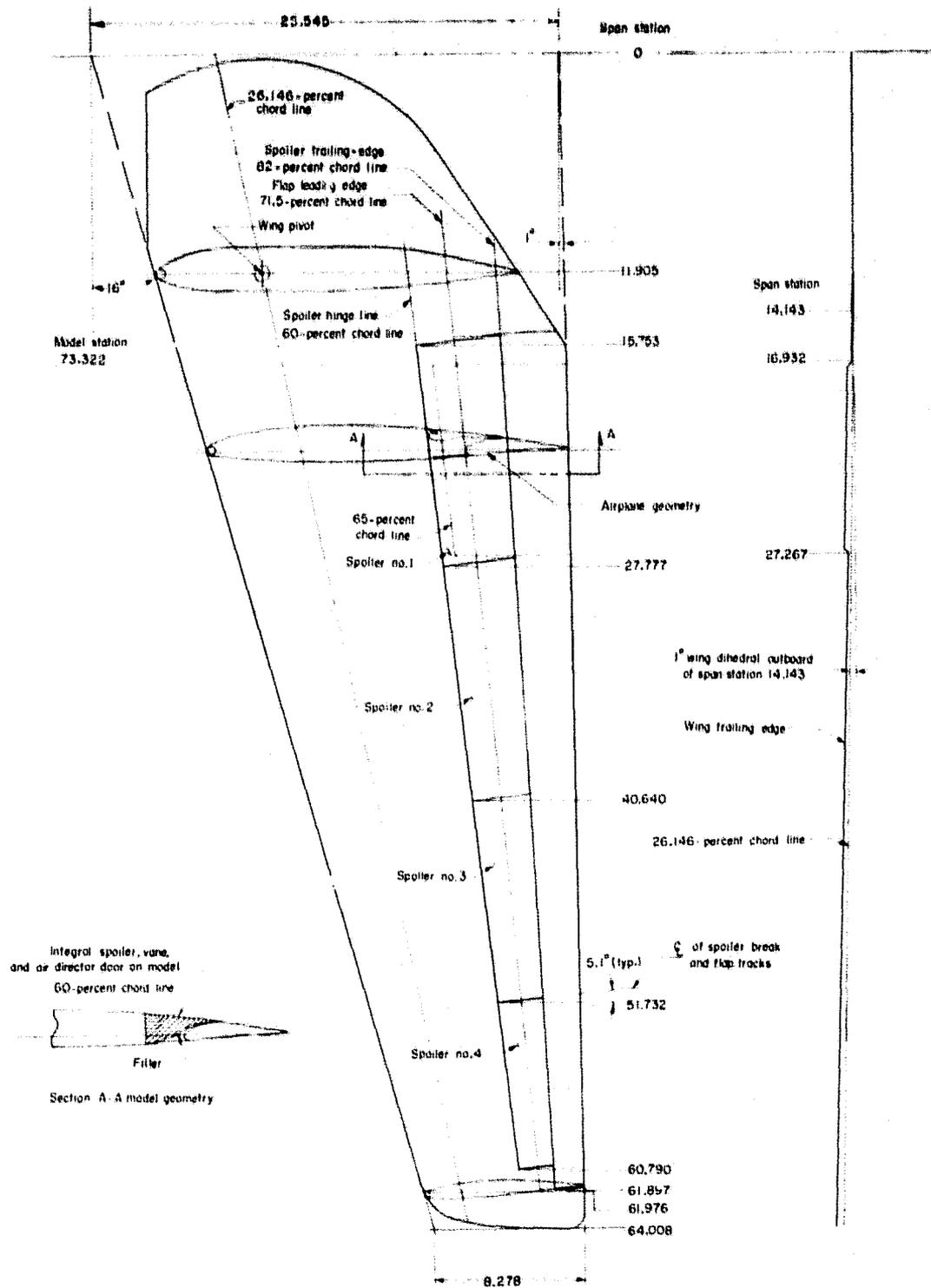
Figure 2.- Wing details. All linear dimensions are in centimeters.

Spoiler

Vane

Air director door

Flap

Basic wing (airplane geometry)

Slotted cruise flap $\delta_{s(1,2,3)} = 3°$ $\delta_{s(4)} = 0°$ $\delta_{ft} = 4°$

Unslotted cruise flap $\delta_{fr} = 4°$

Unslotted cruise flap $\delta_{fr} = 8°$
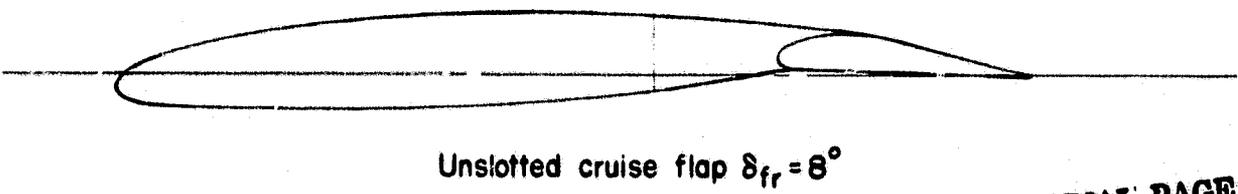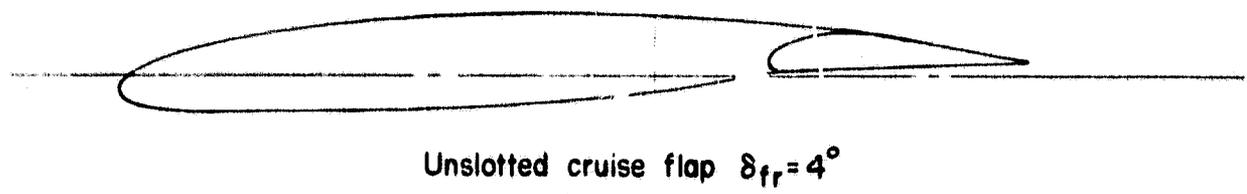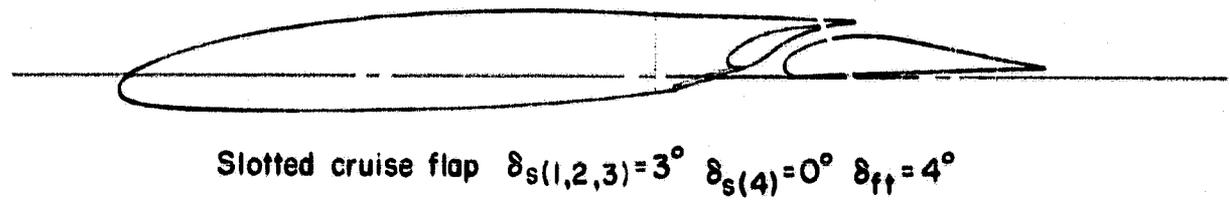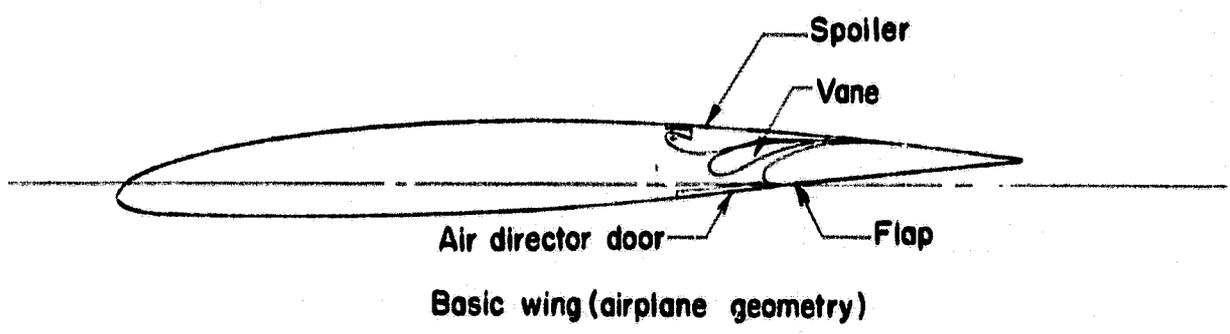
Figure 3.- Flap configurations investigated.
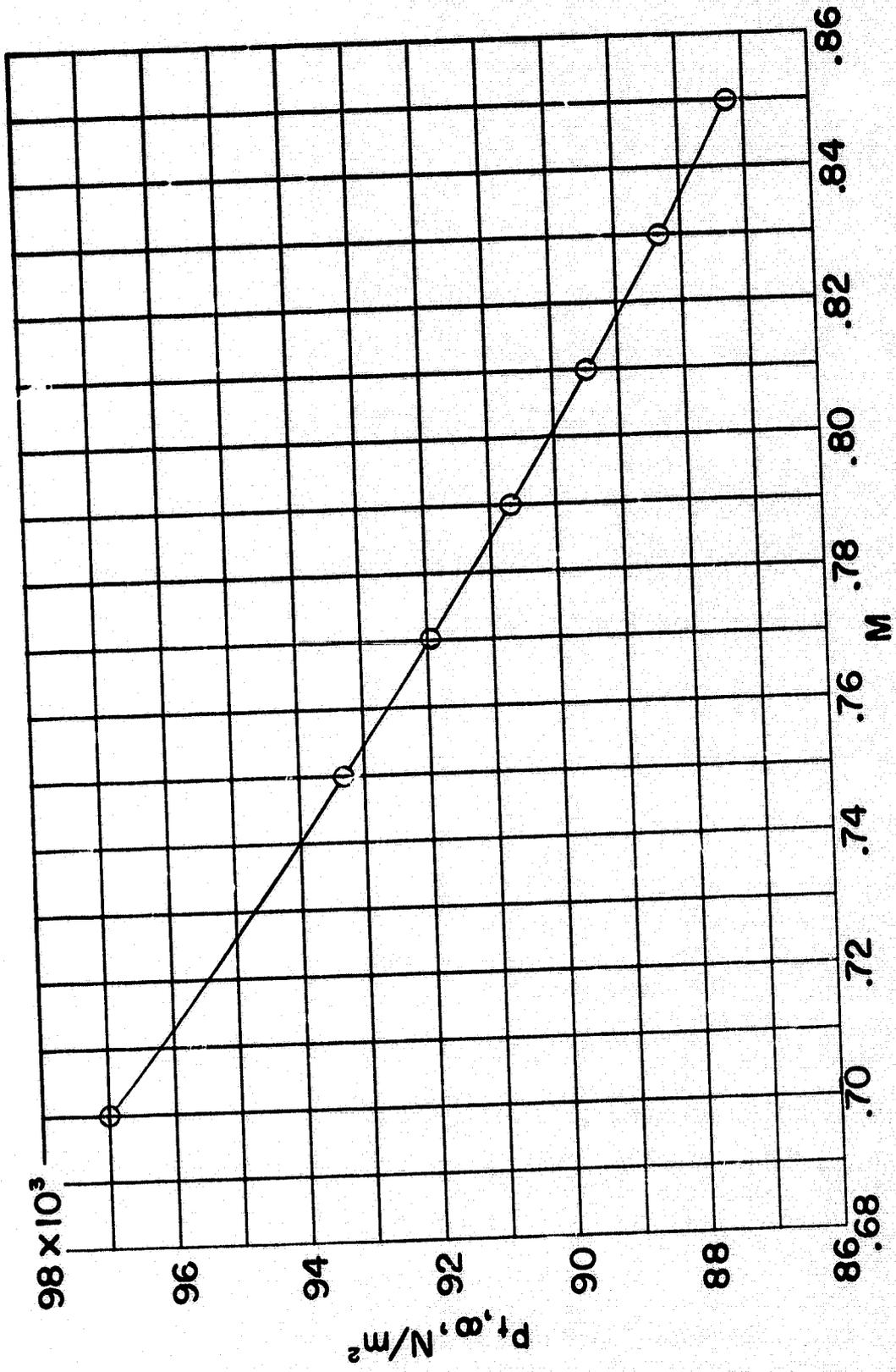
Figure 4.- Variation of the stagnation pressure with Mach number for the investigation in the Langley 8-foot transonic pressure tunnel. Reynolds number per meter, 1.07×10^6; stagnation temperature, 120° F (321.7° K).
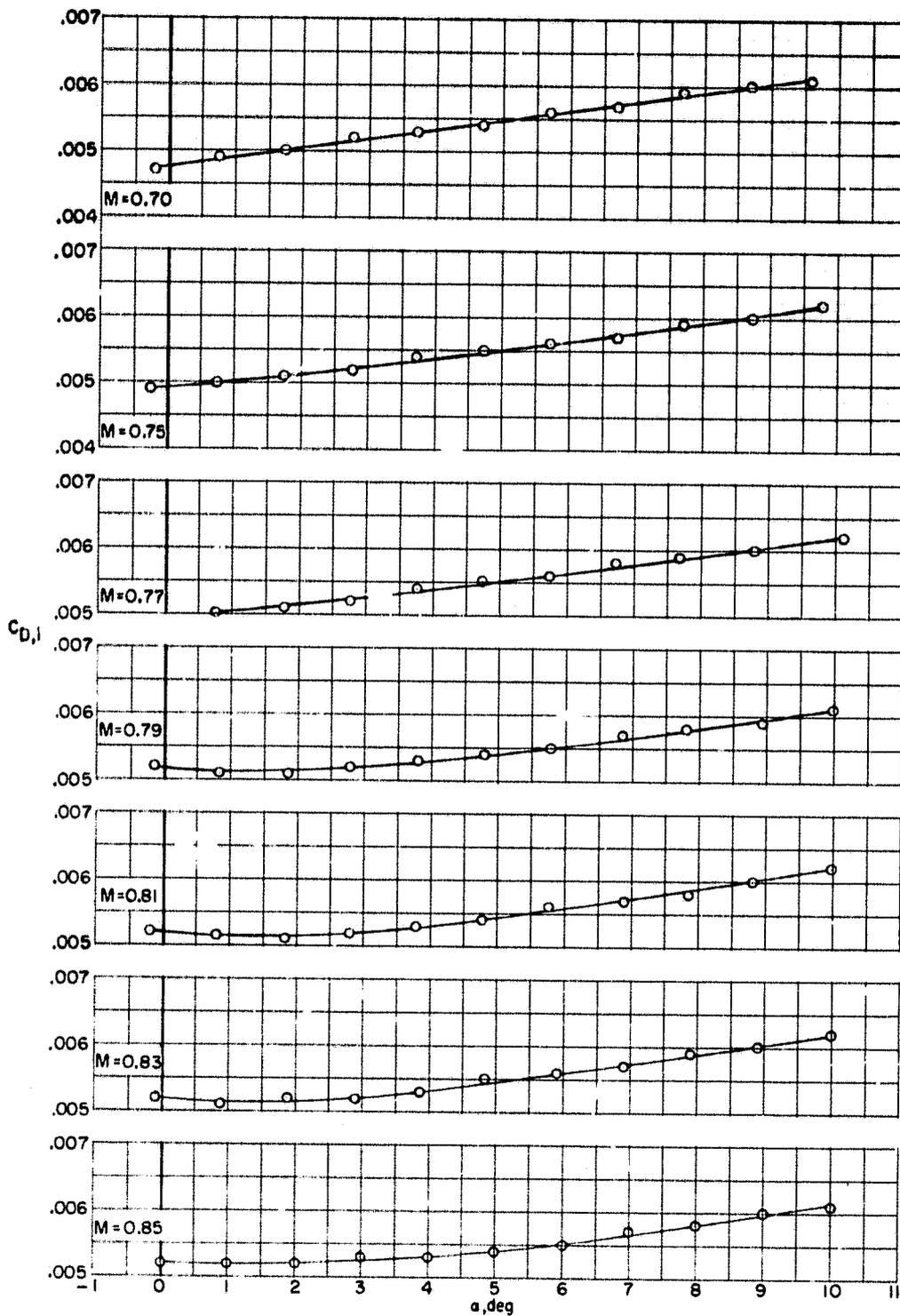
Figure 5.- Variation of internal drag coefficient with Mach number.
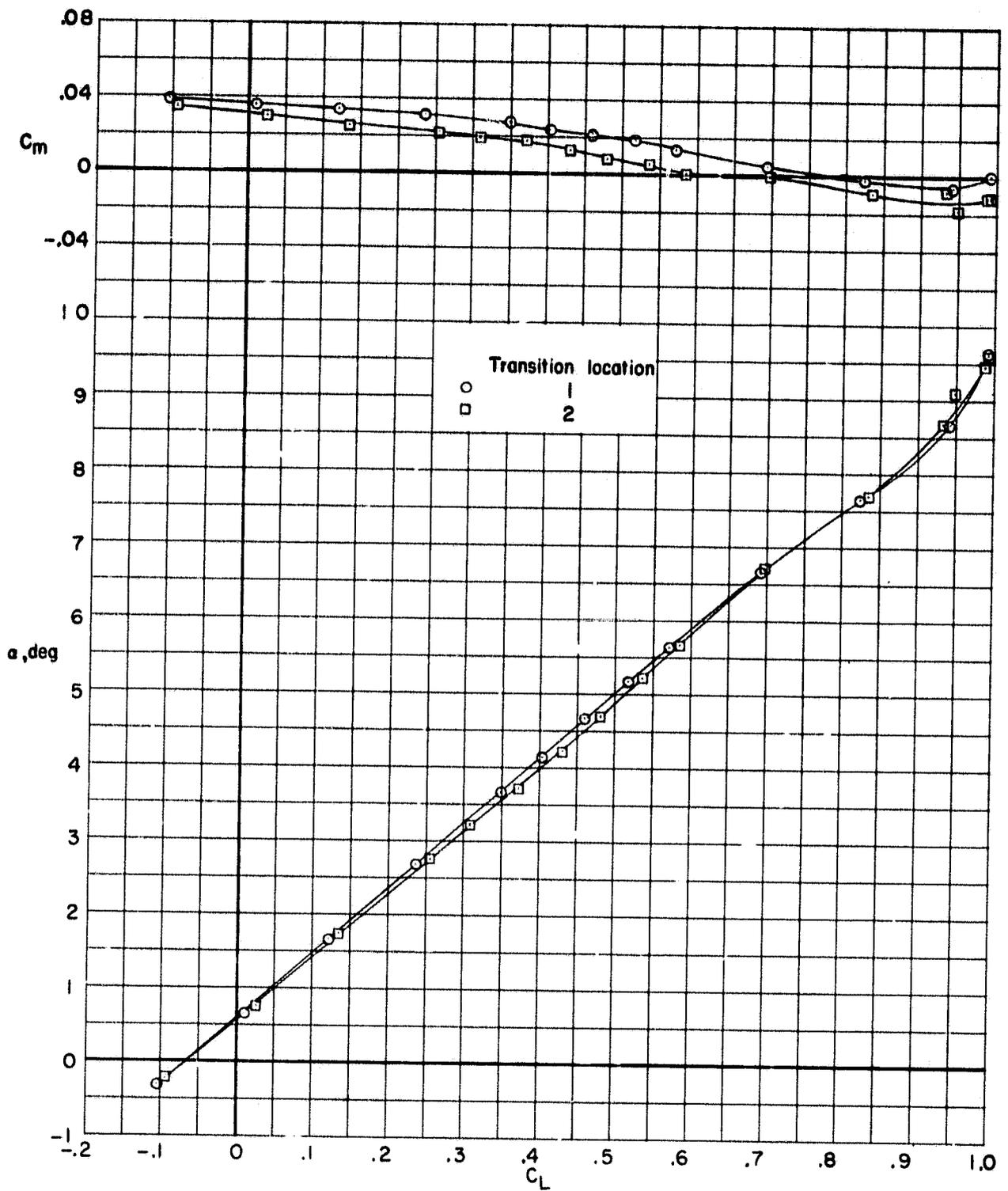
(a) M = 0.70.

Figure 6.- Effect of wing-transition location on the longitudinal aerodynamic characteristics of the basic configuration.

(a) M = 0.70 - Concluded.

Figure 6.- Continued.
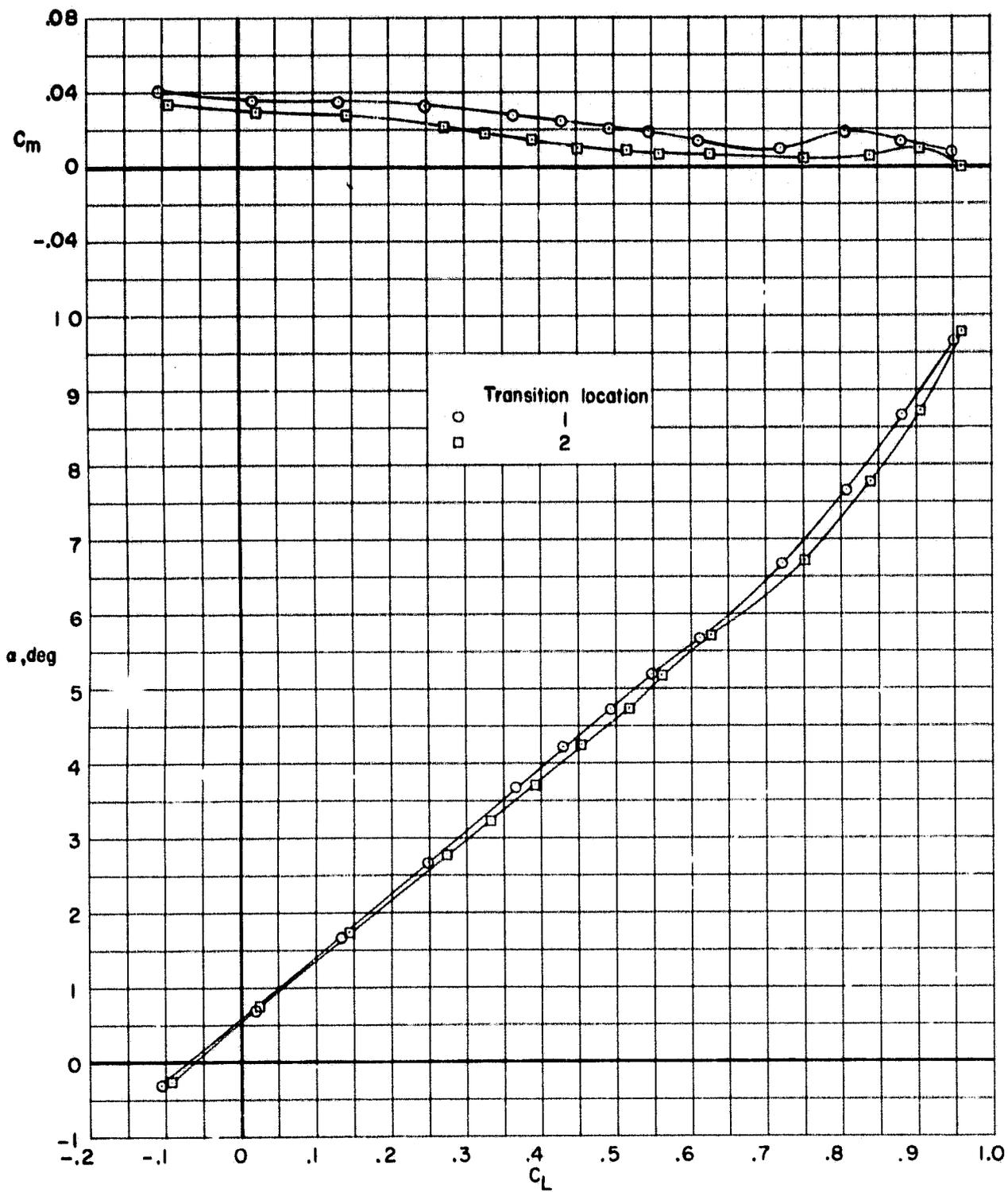
(b) M = 0.75.

Figure 6.- Continued.
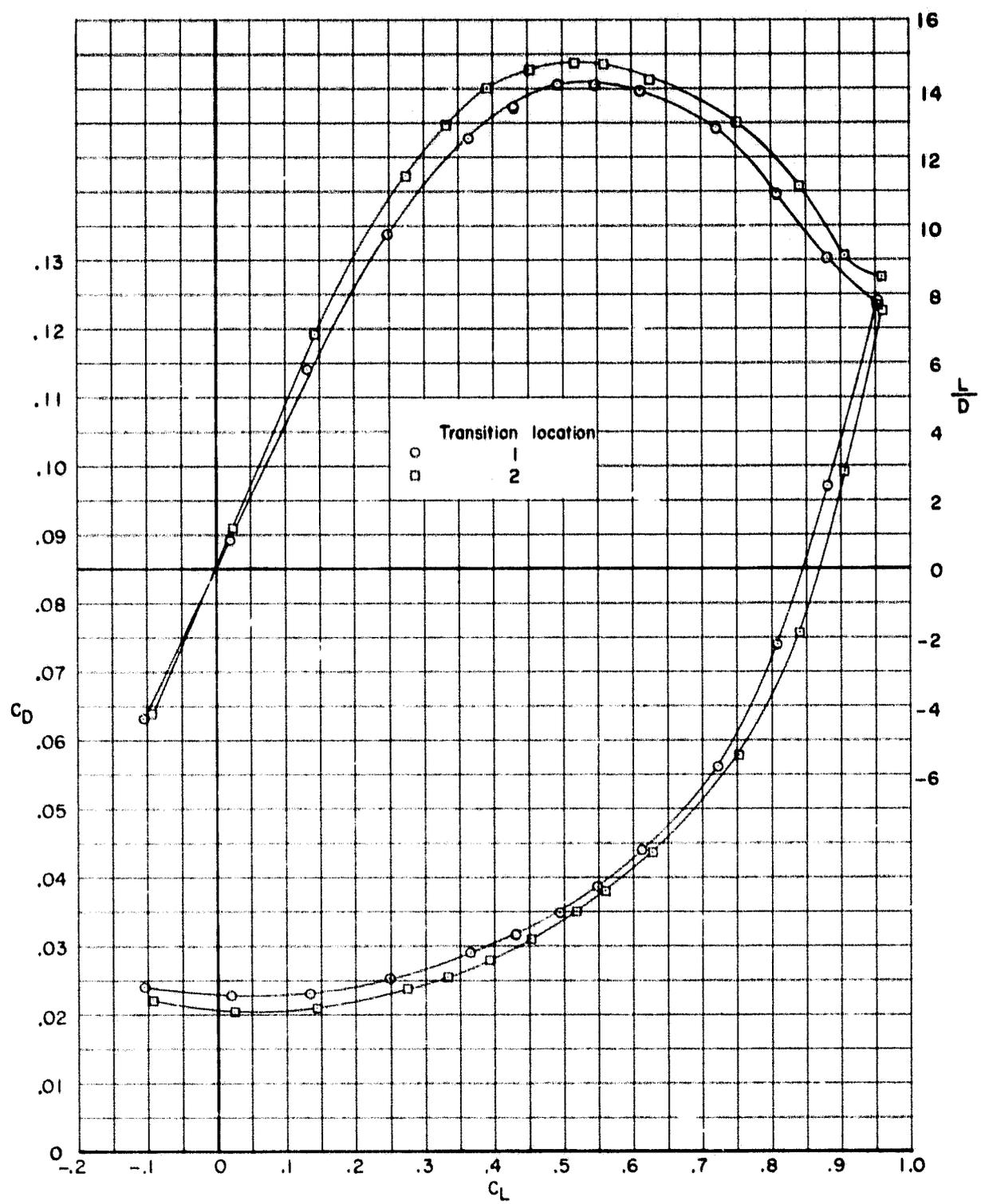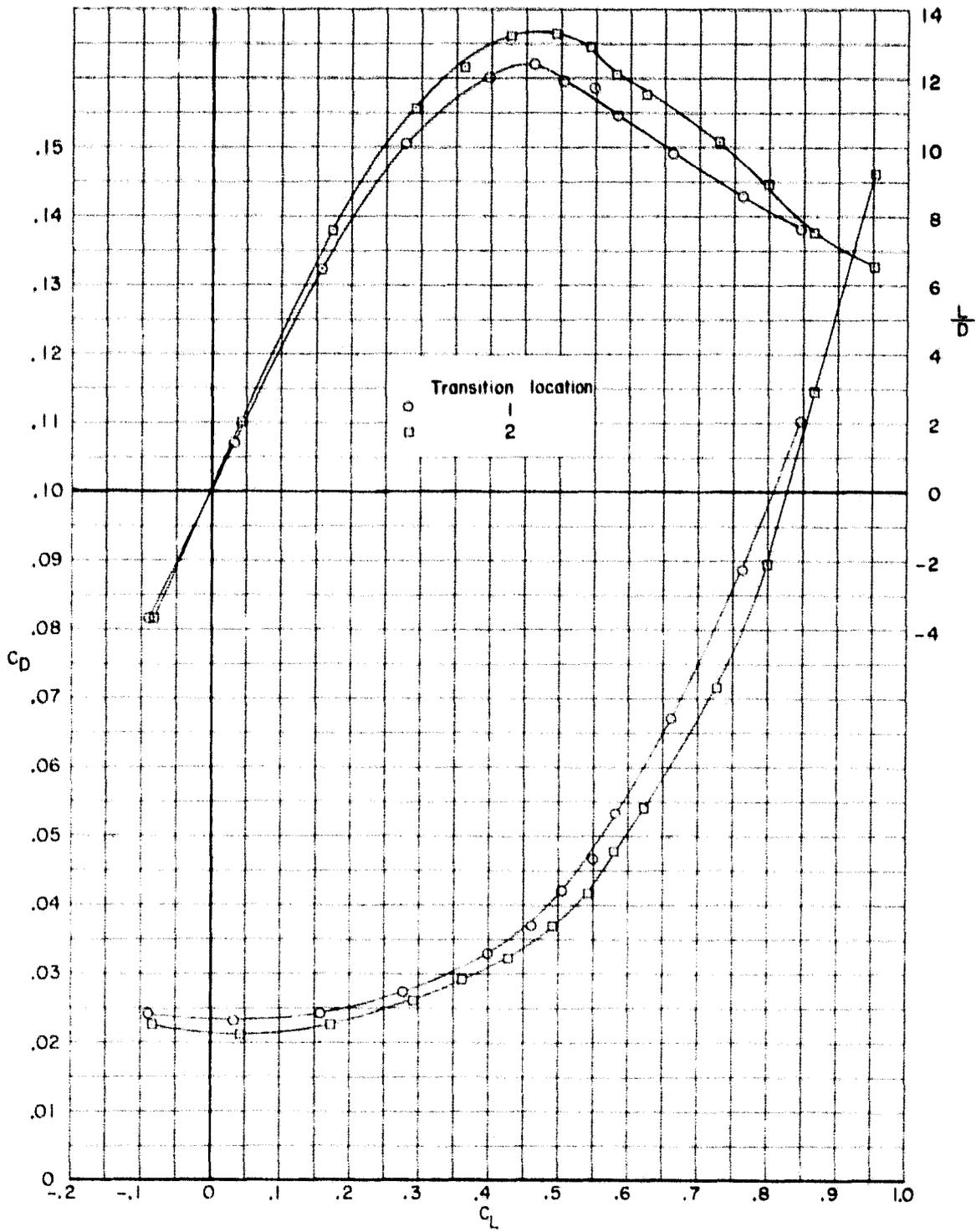
(b) M = 0.75 – Concluded.

Figure 6.– Continued.

(c) M = 0.79.

Figure 6.- Continued.

(c) M = 0.79 - Concluded.
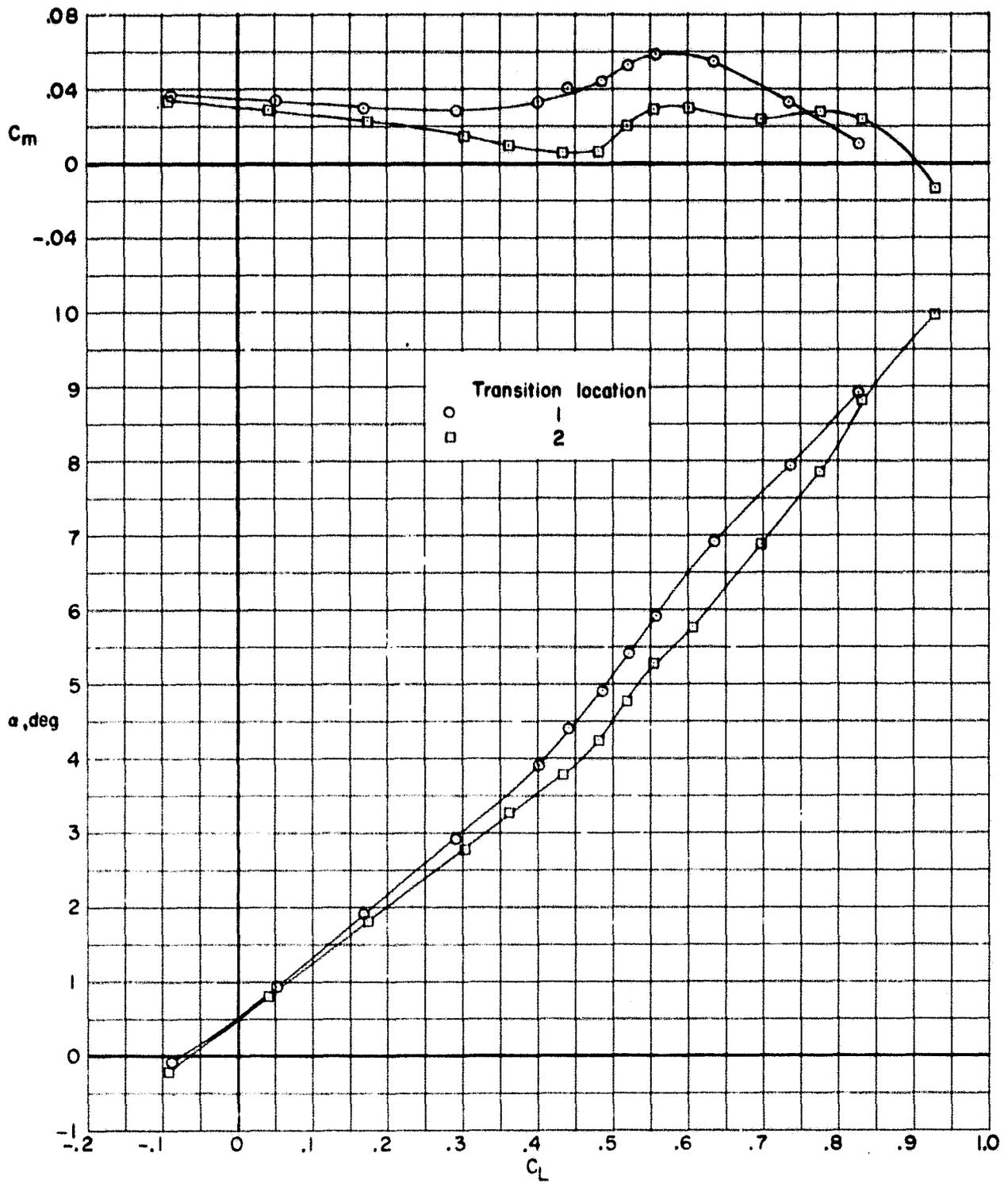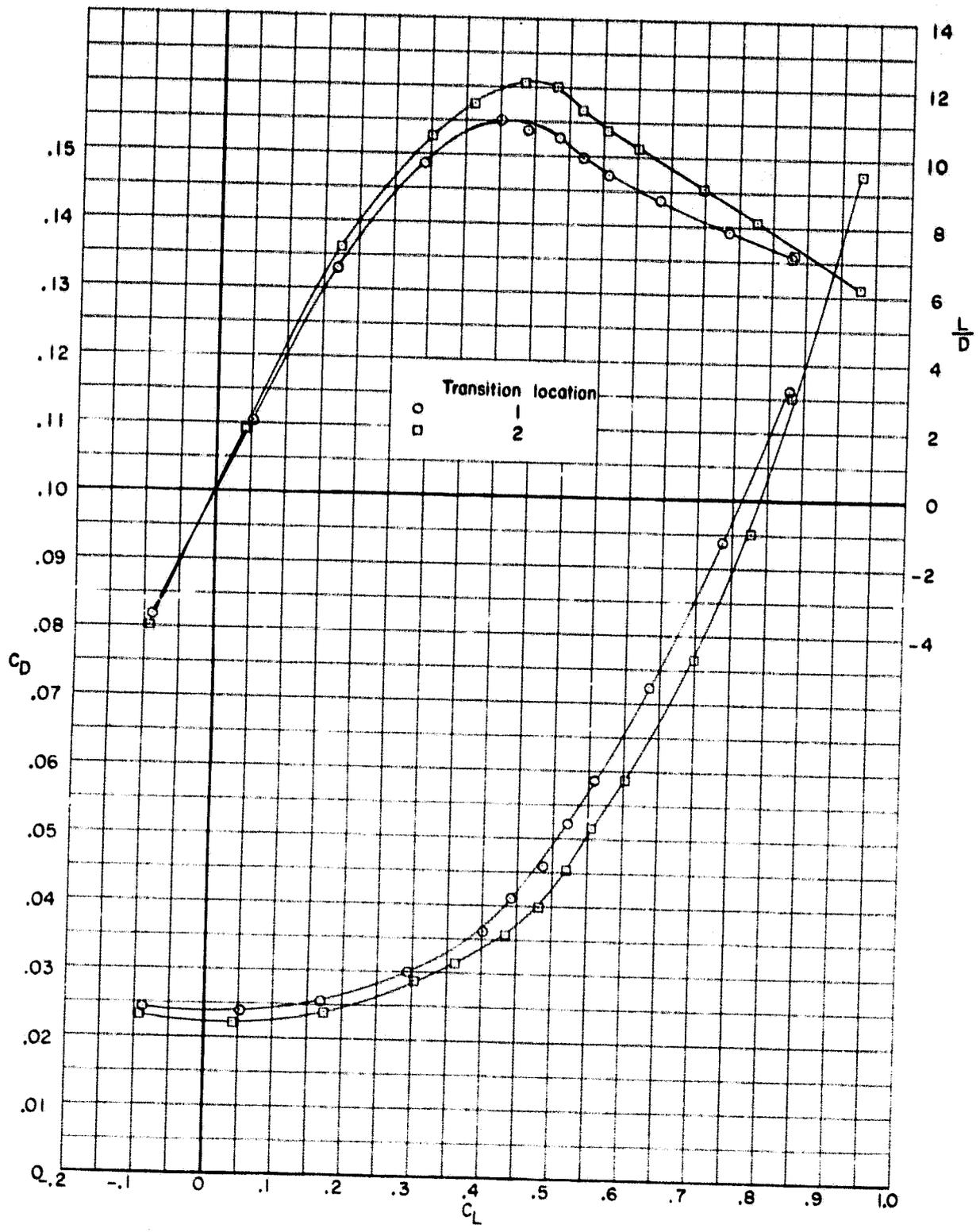
Figure 6.- Continued.

(d) M = 0.81.

Figure 6.- Continued.

(d) M = 0.81 — Concluded.
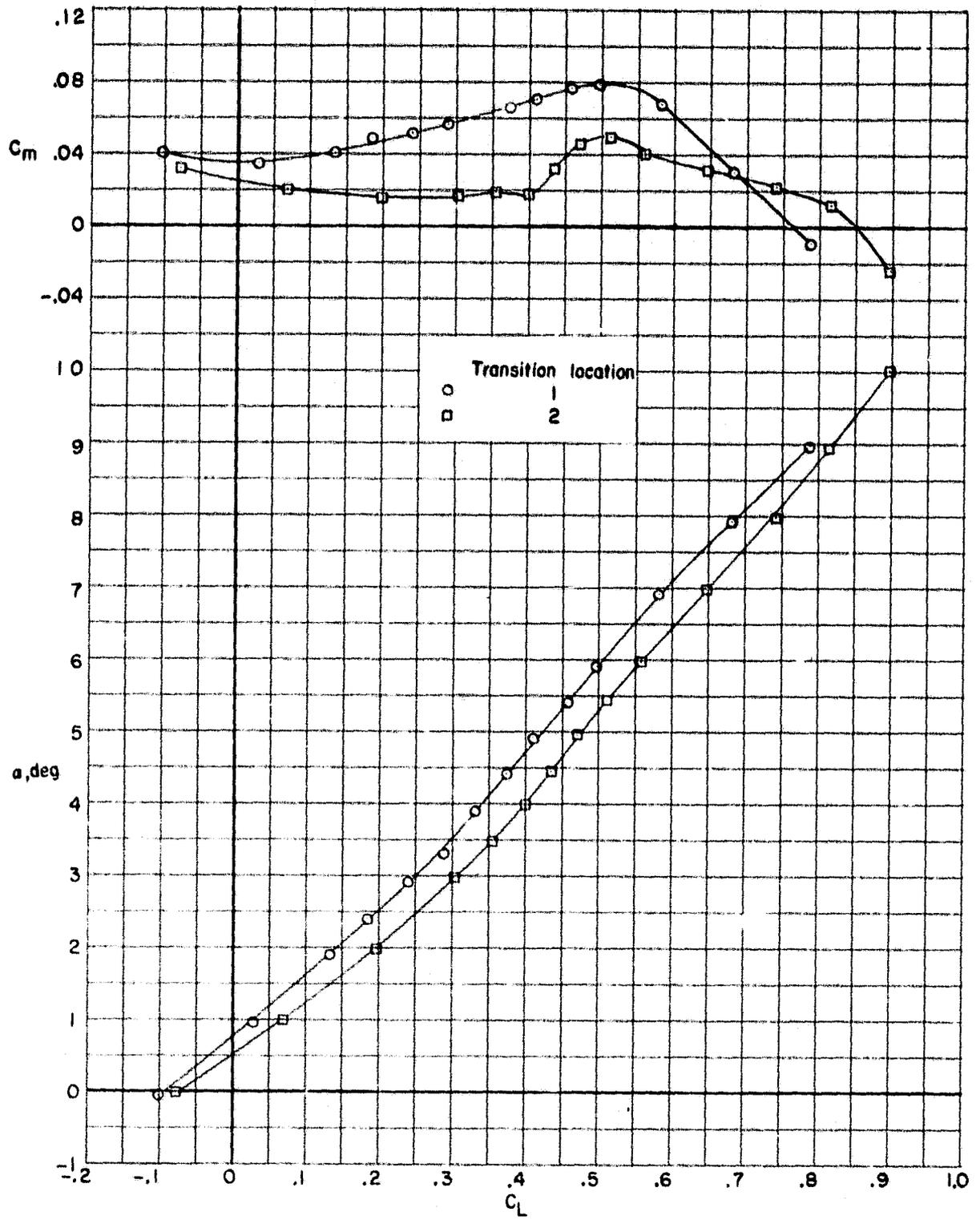
Figure 6.- Continued.

(e) M = 0.85.

Figure 6.- Continued.
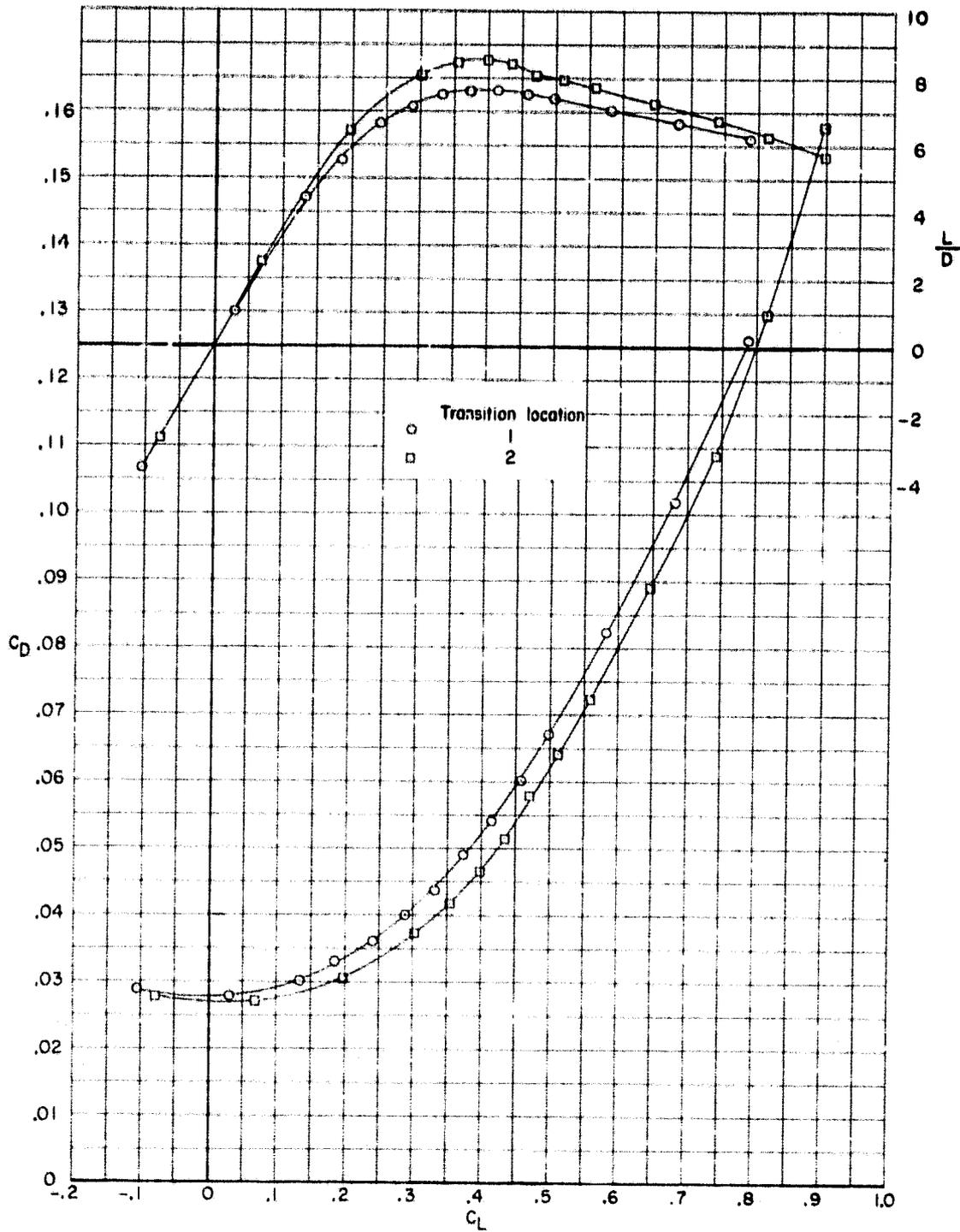
(e) M = 0.85 – Concluded.

Figure 6.- Concluded.
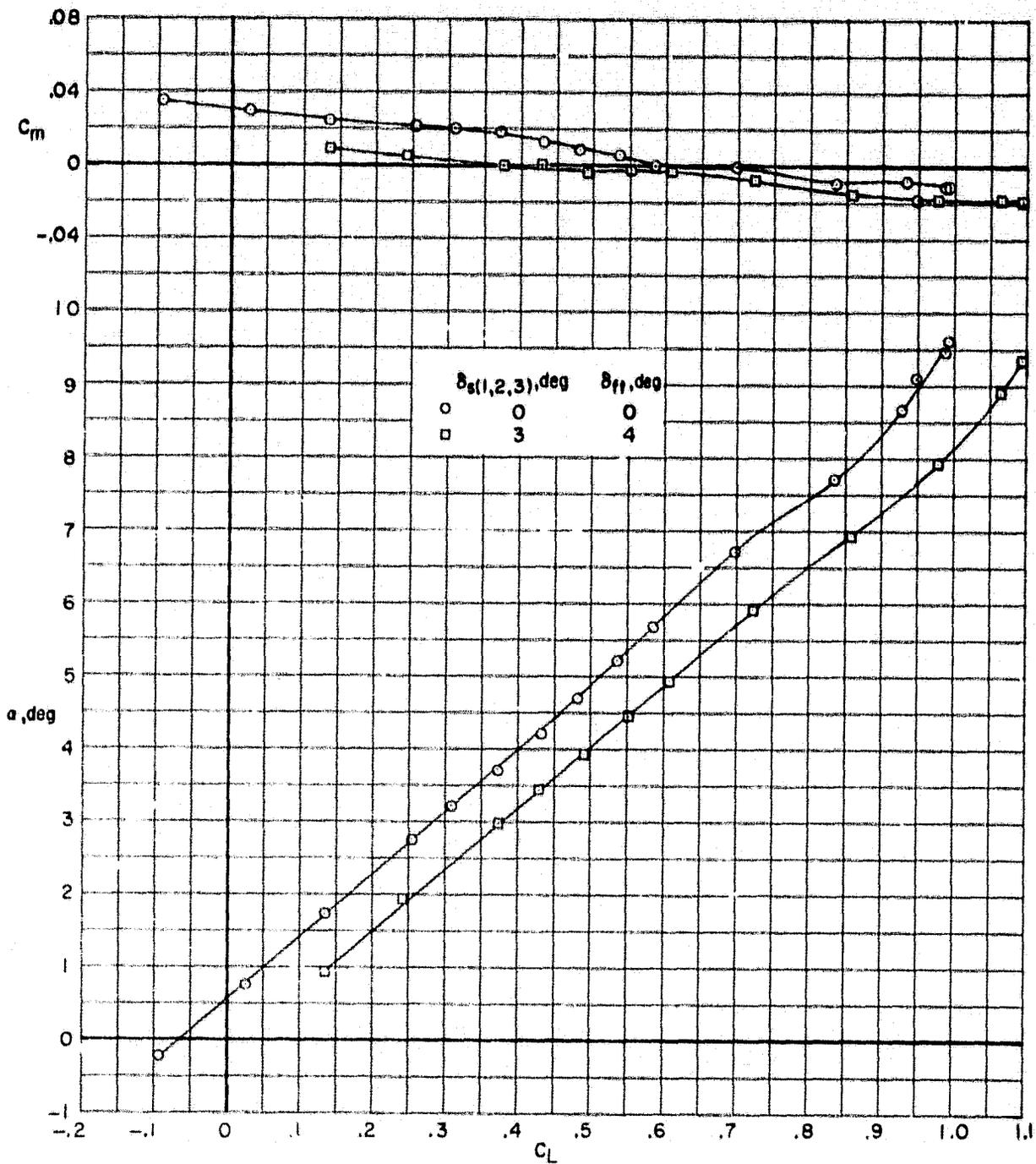
(a) M = 0.70.

Figure 7.- Effect of slotted high-speed cruise flap on the longitudinal aerodynamic characteristics
of the basic configuration with transition location 2.
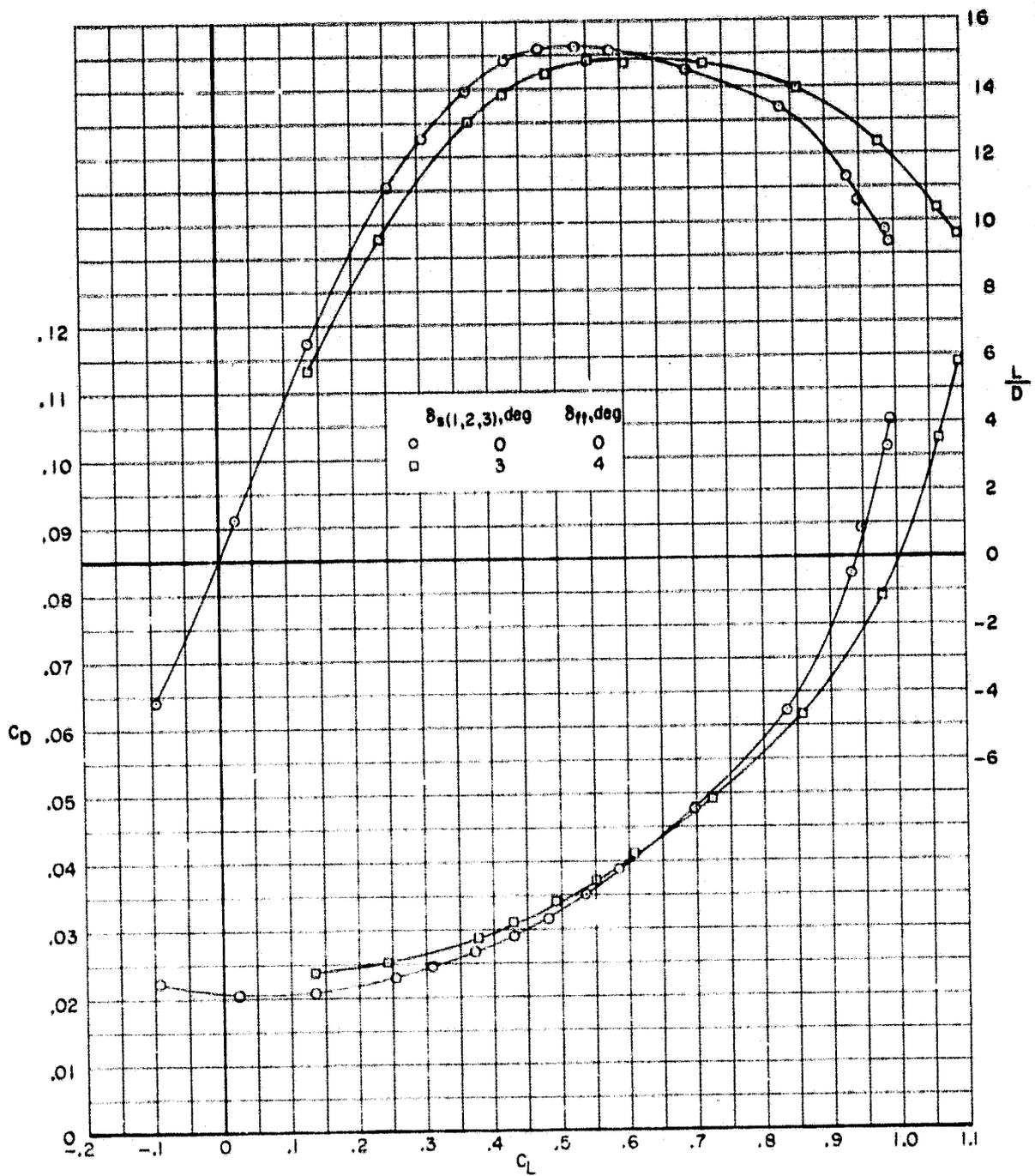
(a) M = 0.70 - Concluded.
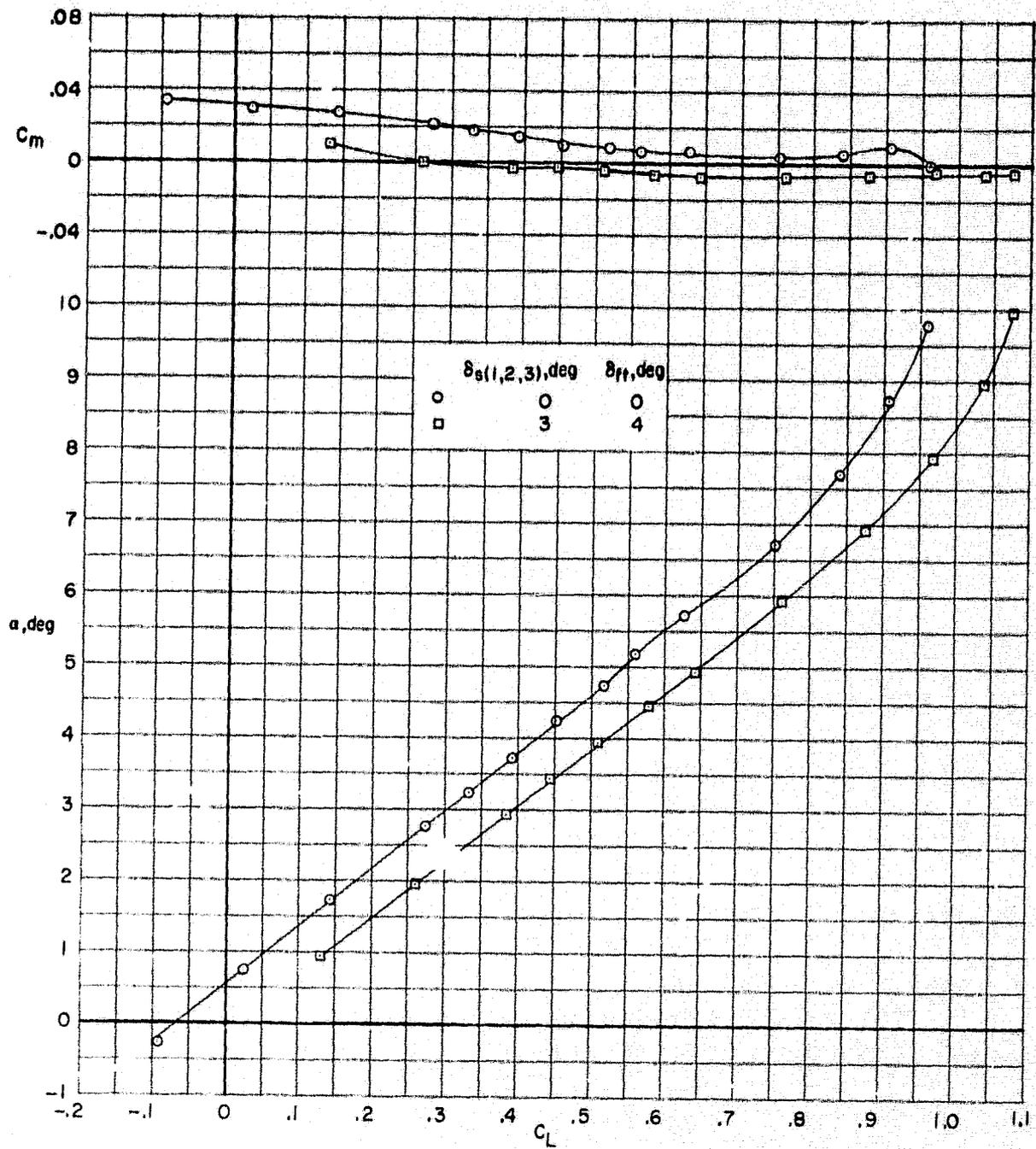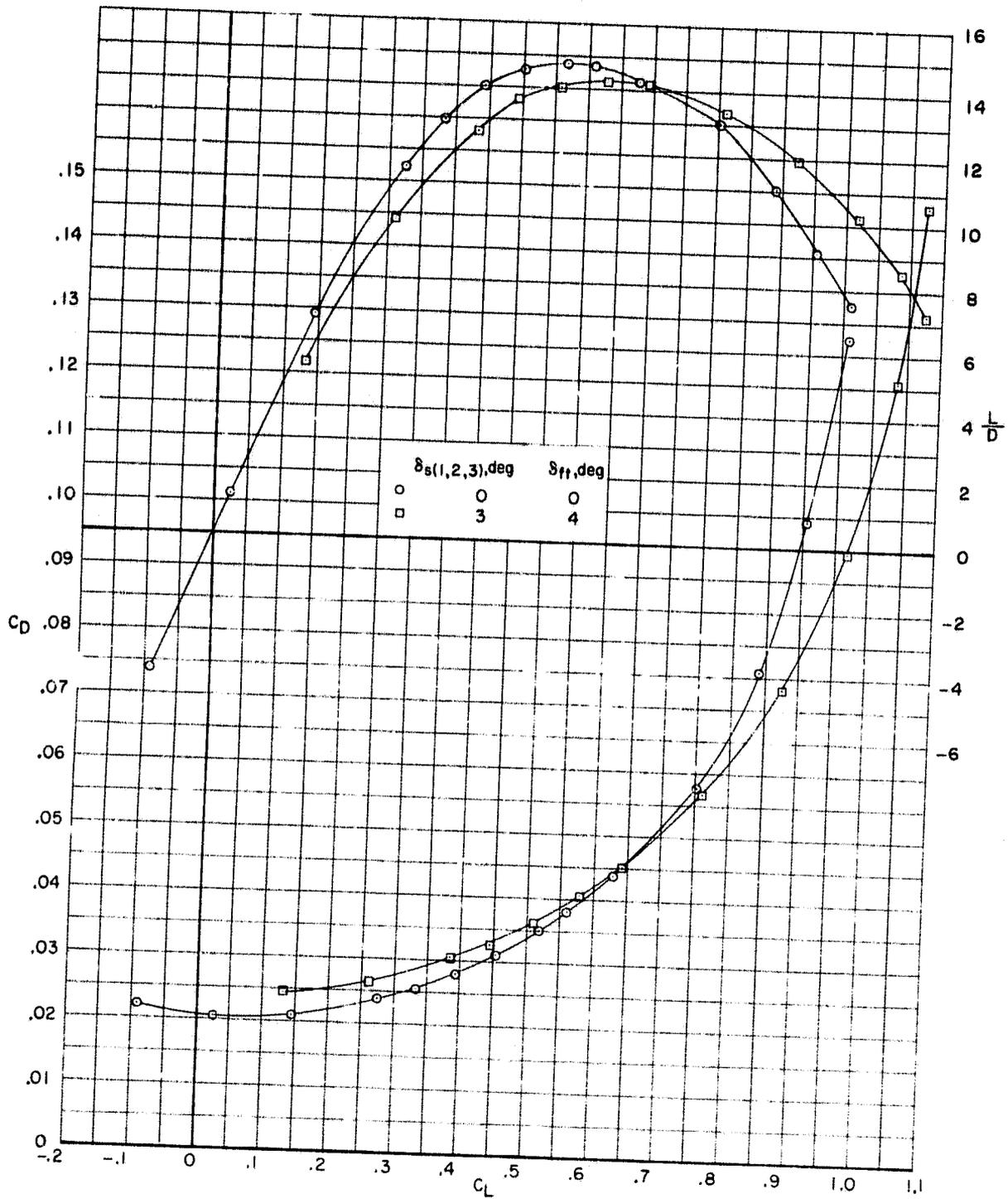
Figure 7.- Continued.

(b) M = 0.75.

Figure 7.- Continued.

(b) M = 0.75 – Concluded.
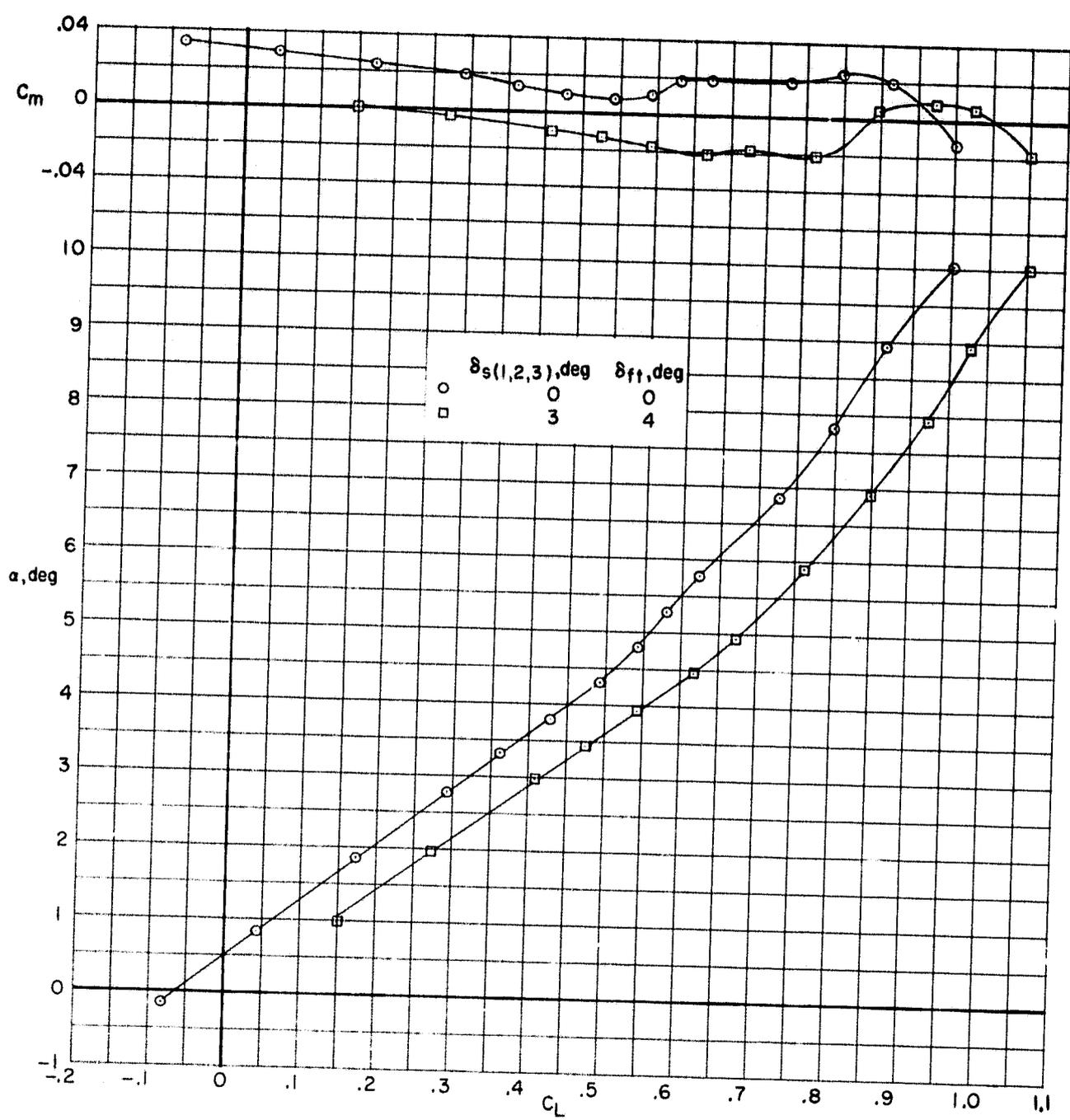
Figure 7.– Continued.

(c) M = 0.79.

Figure 7.- Continued.

(c) M = 0.79 - Concluded.
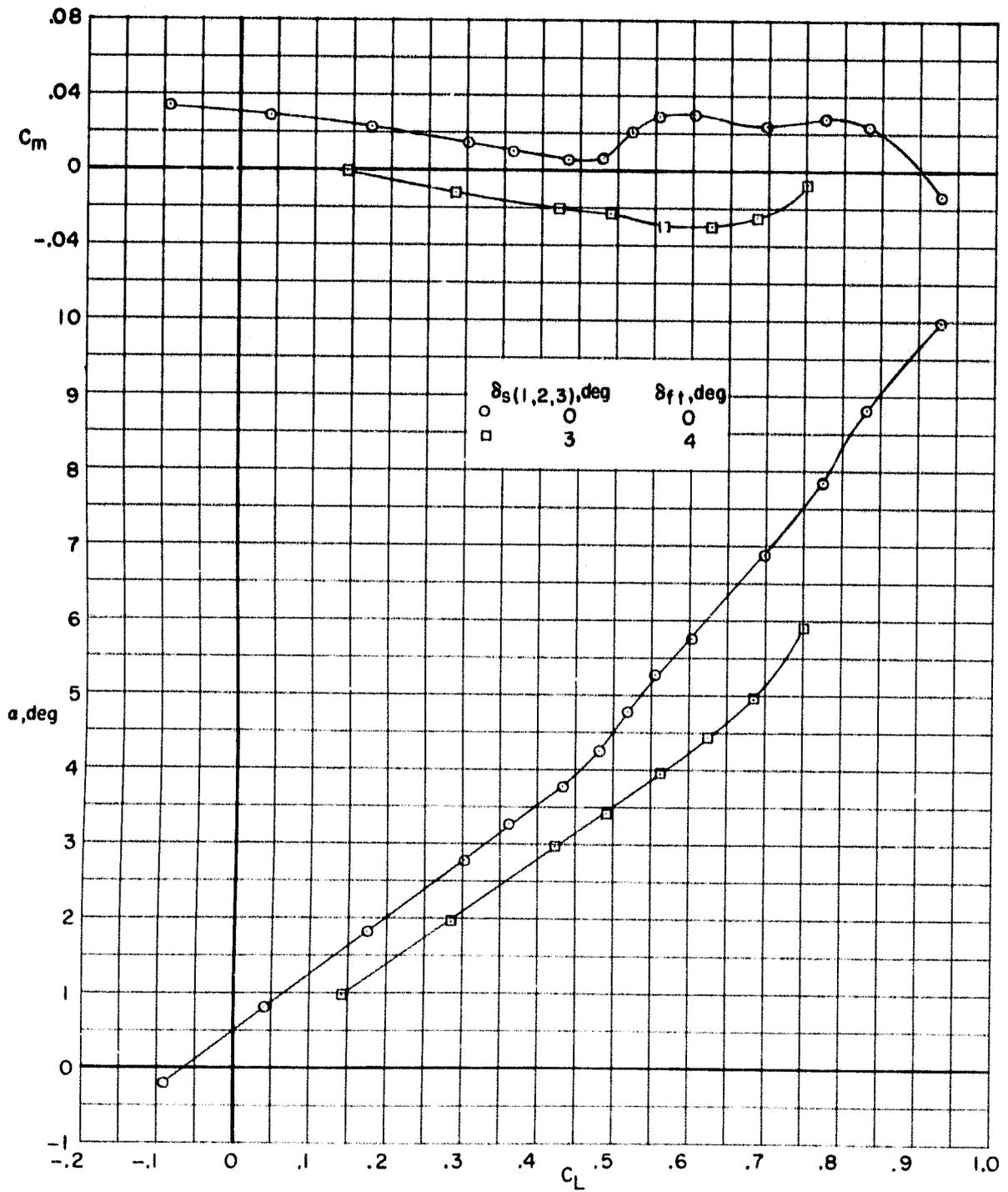
Figure 7.- Continued.

(d) M = 0.81.

Figure 7.- Continued.

(d) M = 0.81 – Concluded.

Figure 7.- Continued.

.08

.04

C_m

0

-.04

$\delta_{s(1,2,3)}$,deg	δ_{ft},deg
○ 0	0
□ 3	4

10

9

8

7

6

a,deg

5

4

3

2

1

0

-1

-.2   0   .1   .2   .3   .4   .5   .6   .7   .8   .9   1.0

C_L

(e) M = 0.83.

Figure 7.- Continued.
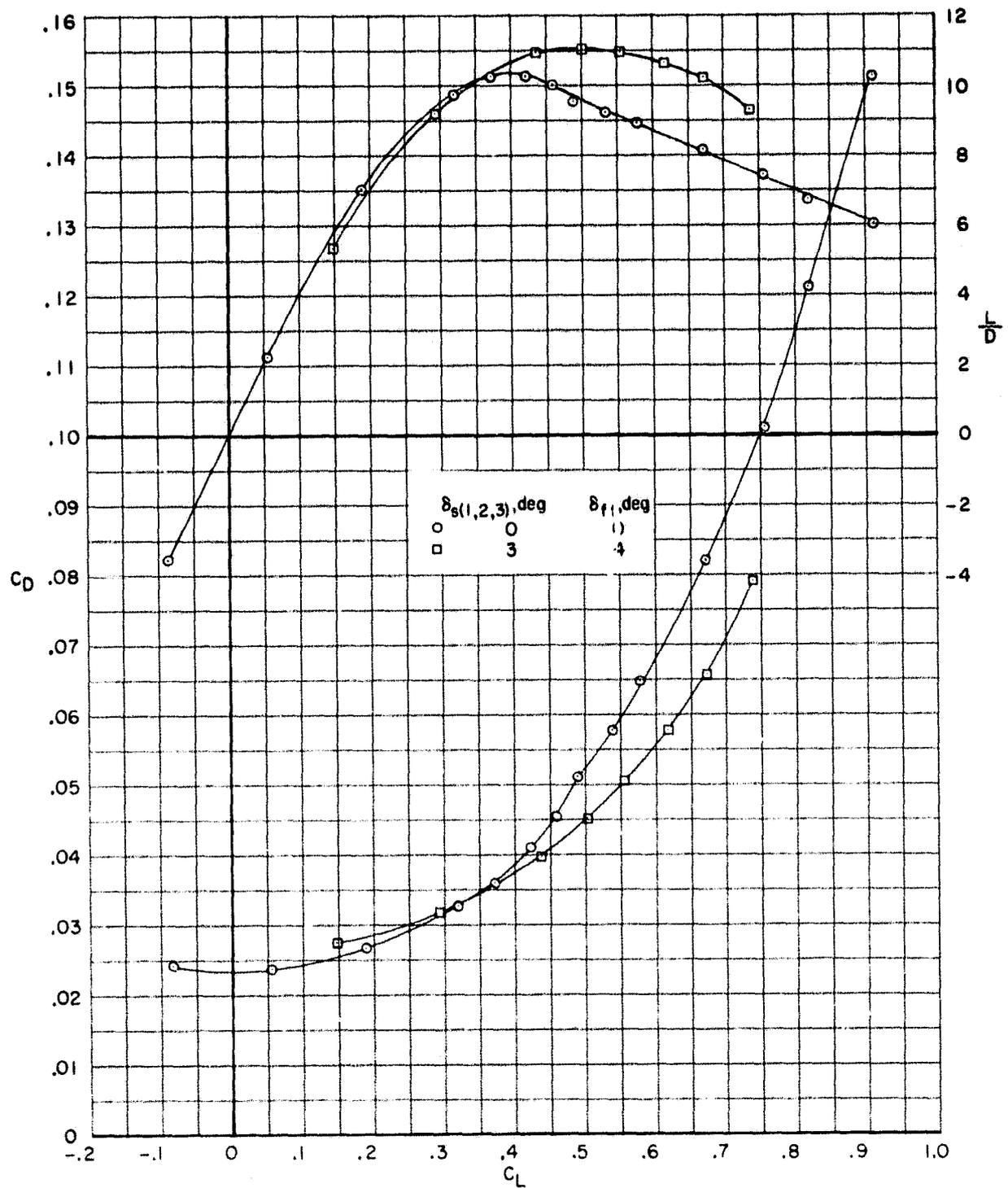
(e) M = 0.83 – Concluded.

Figure 7.- Continued.
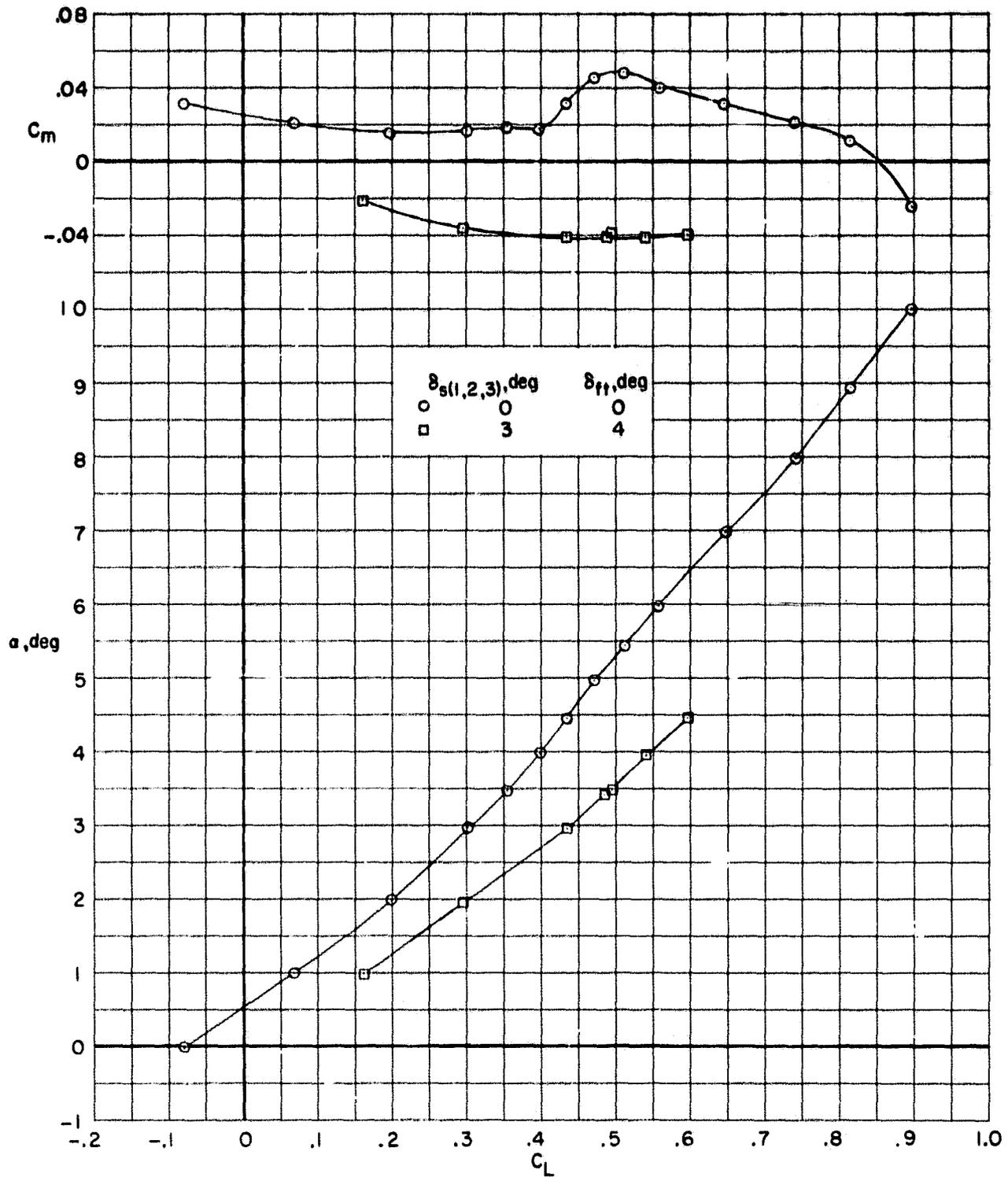
(f) M = 0.85.

Figure 7.- Continued.
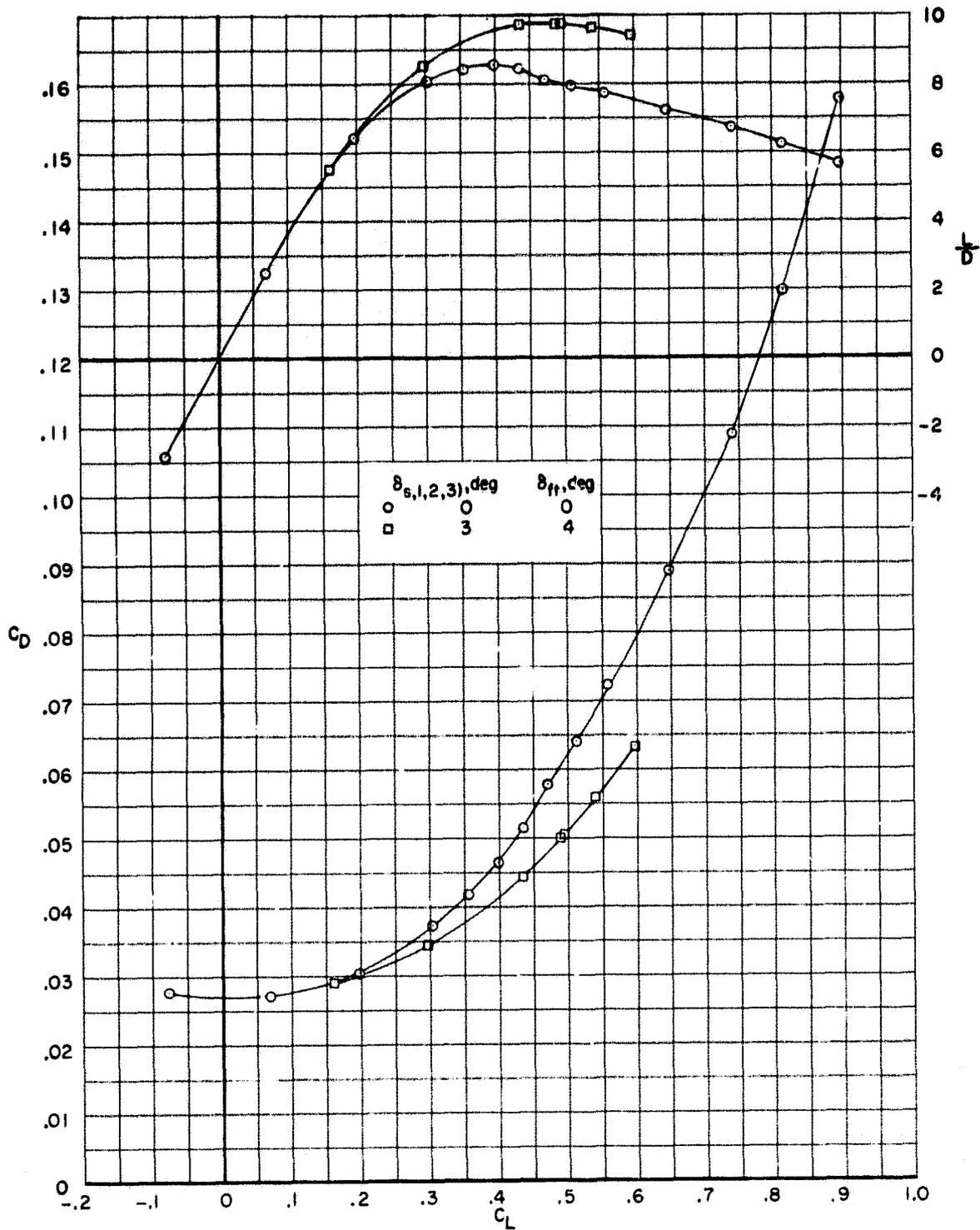
(f) M = 0.85 – Concluded.

Figure 7.- Concluded.
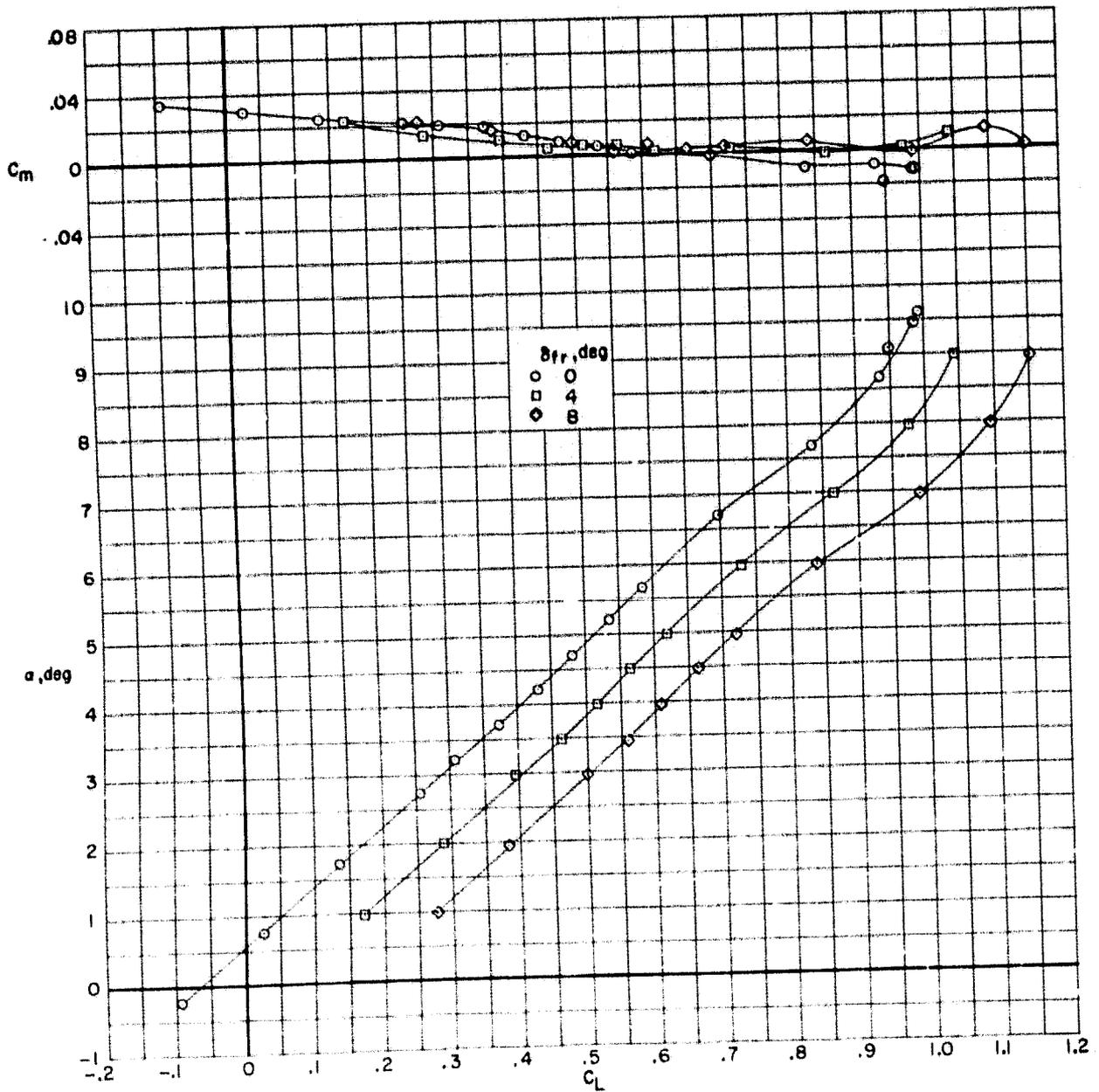
(a) M = 0.70.

Figure 8.- Effect of unslotted high-speed cruise flap on the longitudinal aerodynamic characteristics of the basic configuration with transition location 2.

(a) M = 0.70 - Concluded.
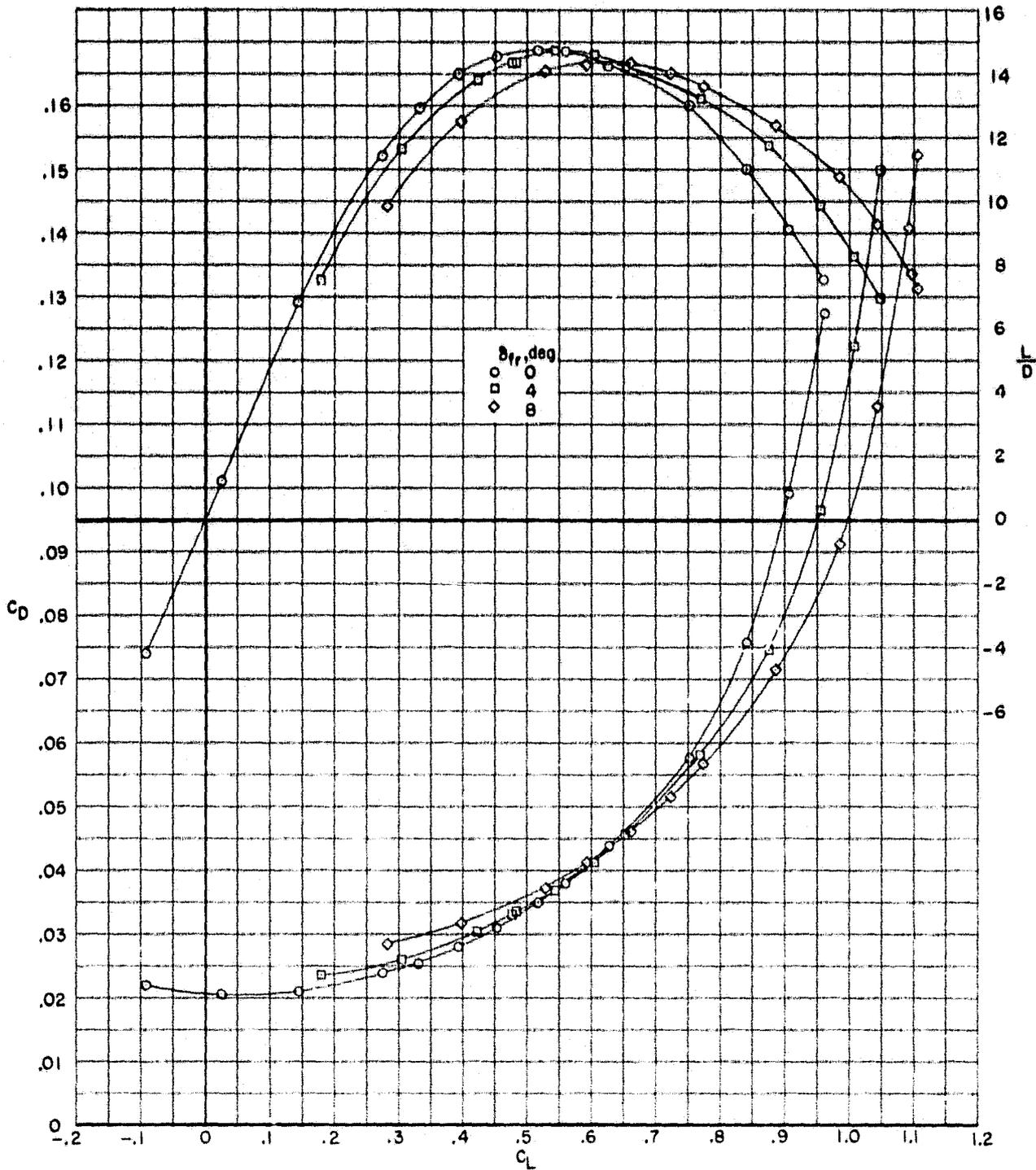
Figure 8.- Continued.

(b) M = 0.75.

Figure 8.- Continued.

(b) M = 0.75 – Concluded.
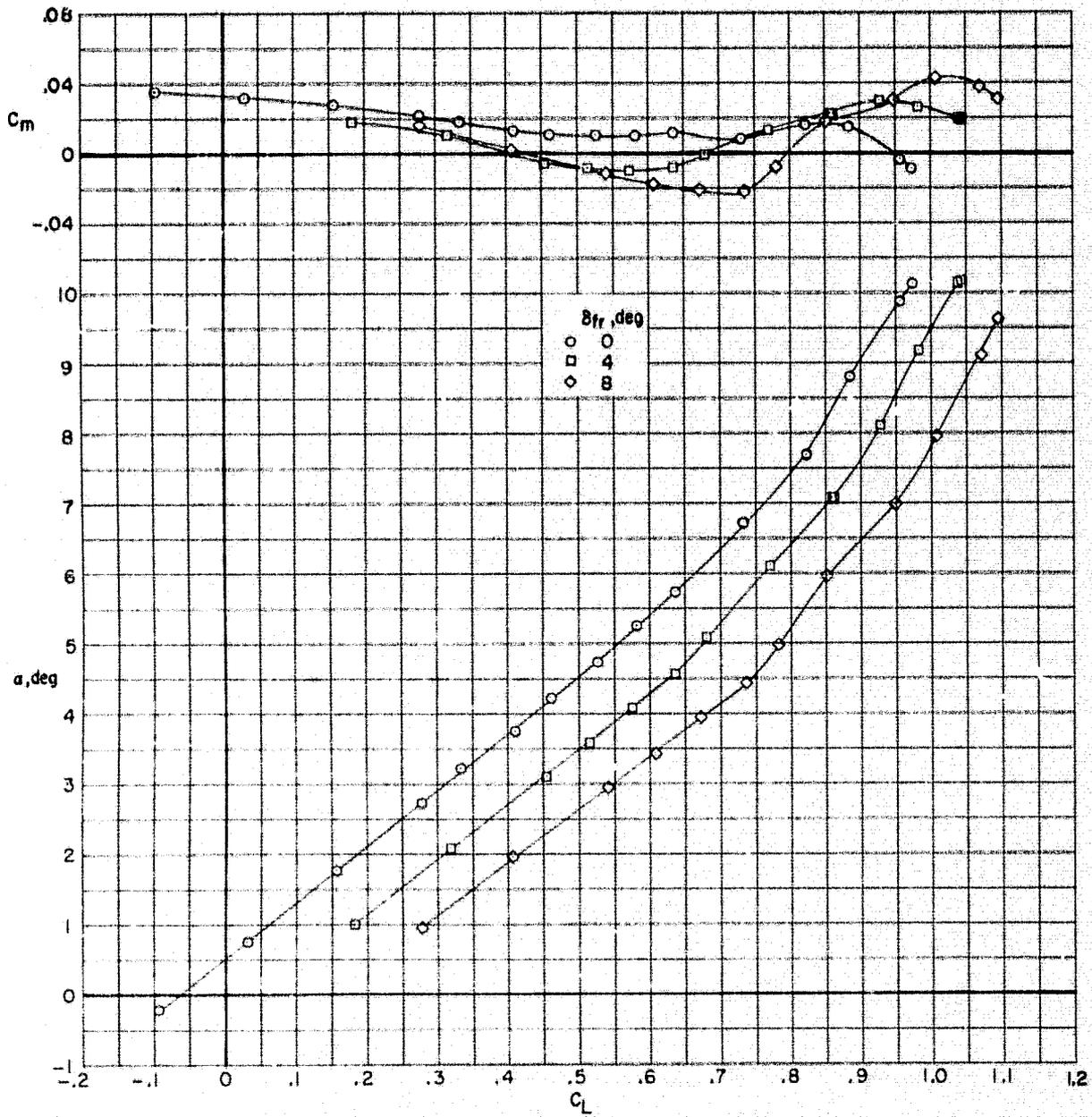
Figure 8.- Continued.

(c) M = 0.77.

Figure 8.- Continued.

(c) M = 0.77 - Concluded.
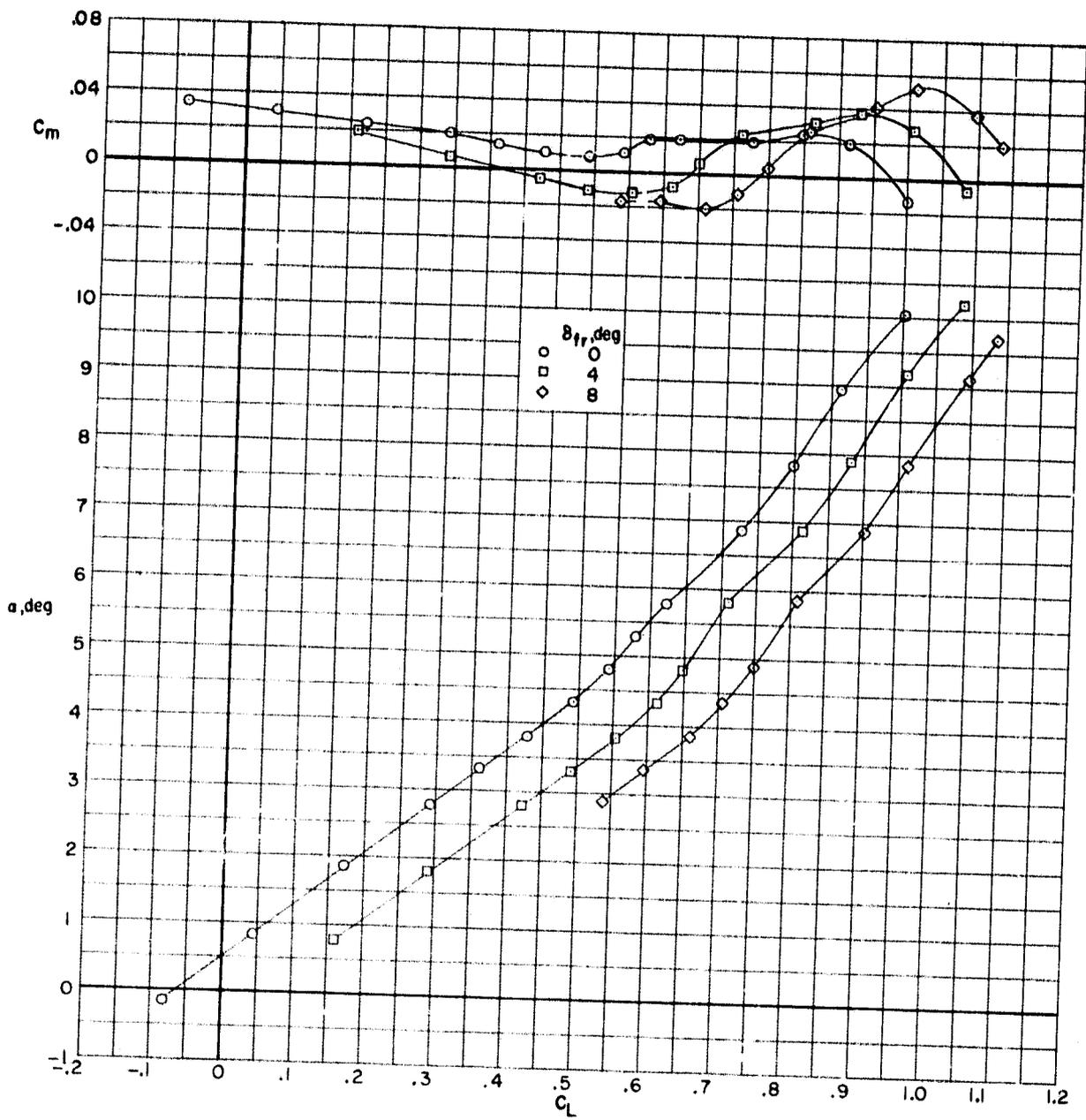
Figure 8.- Continued.

(d) M = 0.79.

Figure 8.- Continued.

(d) M = 0.79 – Concluded.

Figure 8.- Concluded.
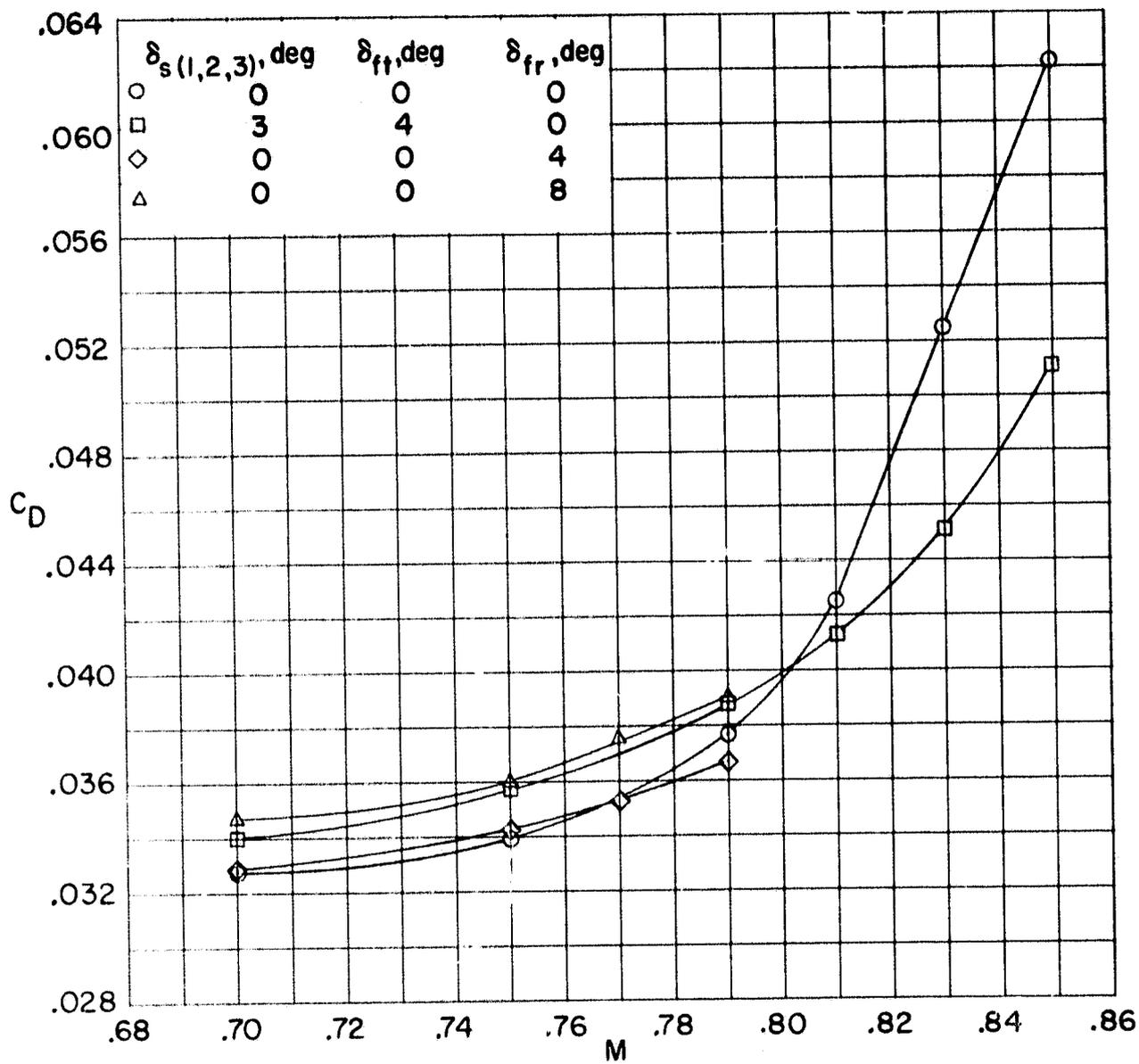
Figure 9.- Effect of cruise flaps on the drag coefficient of the basic configuration with transition location 2. $C_L = 0.5$.
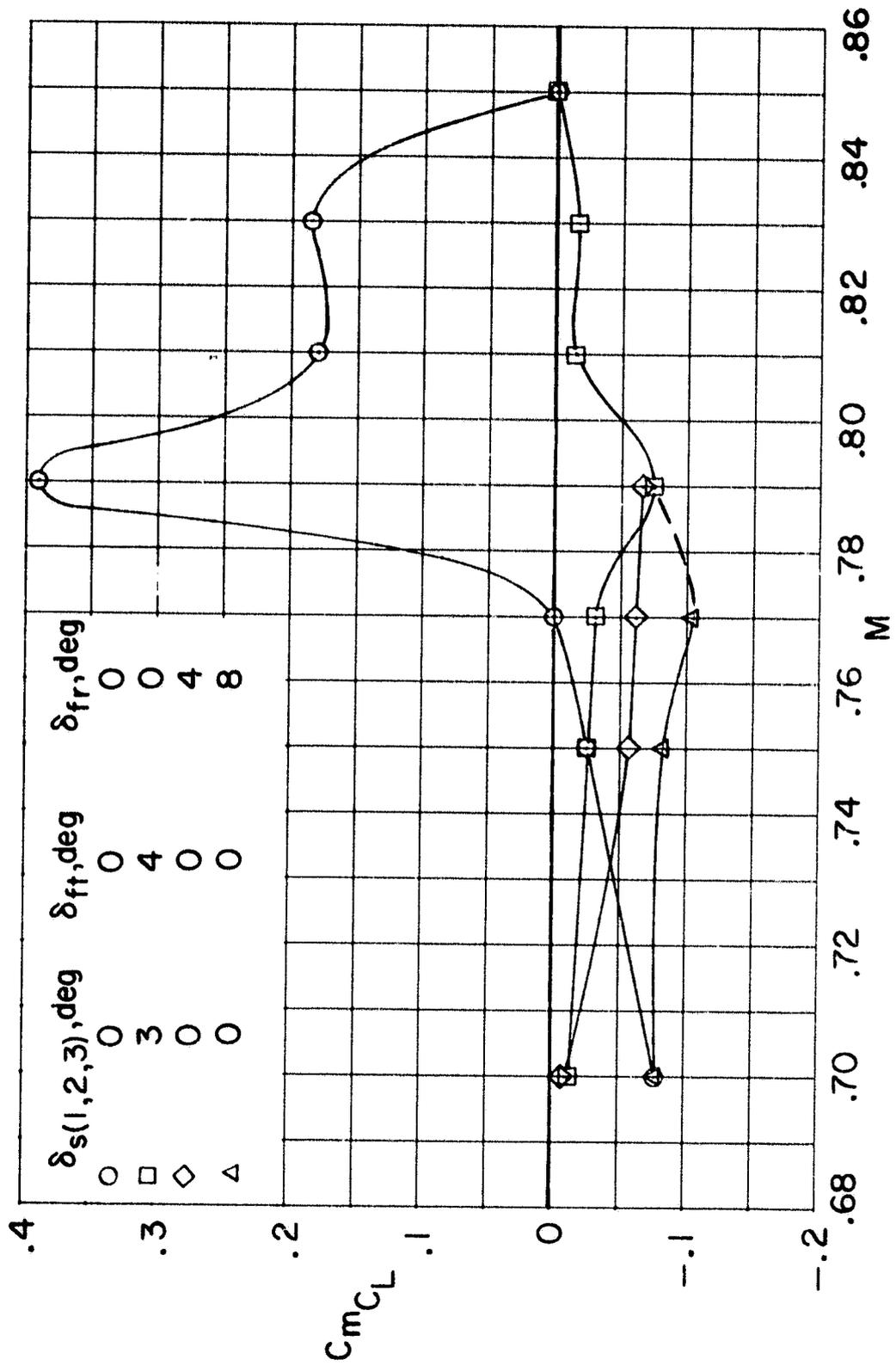
Figure 10.- Effect of cruise flaps on the longitudinal stability derivative of the basic configuration with transition location 2. $C_L \approx 0.5$.